University of Texas Rio Grande Valley
ScholarWorks @ UTRGV

Theses and Dissertations

8-2023

A Preliminary Characterization and Assessment of Mesophotic Octocoral Microbiomes in the Western Gulf of Mexico

Edward P. Gniffke
The University of Texas Rio Grande Valley

Follow this and additional works at: https://scholarworks.utrgv.edu/etd

 Part of the Environmental Sciences Commons, and the Oceanography and Atmospheric Sciences and Meteorology Commons

Recommended Citation

Gniffke, Edward P., "A Preliminary Characterization and Assessment of Mesophotic Octocoral Microbiomes in the Western Gulf of Mexico" (2023). *Theses and Dissertations*. 1280.
https://scholarworks.utrgv.edu/etd/1280

This Thesis is brought to you for free and open access by ScholarWorks @ UTRGV. It has been accepted for inclusion in Theses and Dissertations by an authorized administrator of ScholarWorks @ UTRGV. For more information, please contact justin.white@utrgv.edu, william.flores01@utrgv.edu.

A PRELIMINARY CHARACTERIZATION AND ASSESSMENT OF MESOPHOTIC OCTOCORAL MICROBIOMES IN THE WESTERN GULF OF MEXICO

A Thesis

By

EDWARD (TED) GNIFFKE

Submitted in Partial Fulfillment of the

Requirements for the Degree of

MASTER OF SCIENCE

Major Subject: Ocean, Coastal, and Earth Studies

The University of Texas Rio Grande Valley

August 2023

A PRELIMINARY CHARACTERIZATION AND ASSESSMENT OF MESOPHOTIC OCTOCORAL MICROBIOMES IN THE WESTERN GULF OF MEXICO

A Thesis
By
EDWARD (TED) GNIFFKE

COMMITTEE MEMBERS

Dr. Erin E. Easton
Chair of Committee

Dr. Keir Macartney
Committee Member

Dr. Christopher Gabler
Committee Member

Dr. David Hicks
Committee Member

August 2023

Copyright 2023 Edward Gniffke

All Rights Reserved

ABSTRACT

Gniffke, Edward., A Preliminary Characterization and Assessment of Mesophotic Octocoral Microbiomes in the western Gulf of Mexico. Master of Science (MS), August, 2023, 83 pp., 10 tables, 16 figures, references, 122 titles.

Mesophotic Coral Ecosystems are highly diverse and productive ecosystems in the western Gulf of Mexico which are composed of, in part, by octocorals (subclass Octocorallia). Despite their importance as foundational organisms octocorals are an understudied group in this region, with little known about their microbial community. Ninety-eight Octocoral samples collected from the western and northwestern Gulf of Mexico were sequenced using *16S* rRNA sequencing to characterize their microbial communities. The sequenced microbiomes were generally low in diversity composed of a few core microbial taxa. Octocoral group was the main driver of microbiome composition as opposed to depth, season, region, and reef type. The effect of sequencing depth on a subset of 24 samples was examined, and showed low sequencing depth was sufficient to capture microbiome community trends. This microbiome data may be used to improve our understanding of the biology of octocorals in the Gulf of Mexico and contribute to conservation efforts in the future.

DEDICATION

To my mother, Keiko Gniffke, who never stopped encouraging me to pursue my passions and to my sister, Erika Gniffke, who was a constant source of support. Thank you for believing in my impulsive ideas. To my loving partner, Maggie Seida, thank you for bringing me joy and a shared connection to the ocean that brought us together.

ACKNOWLEDGMENTS

The patience and support of my advisor and thesis committee chair, Dr. Erin Easton, was critical in allowing me to learn a new field of study and perform this thesis research on it in a timely manner. The assistance of Dr. Keir Macartney was also crucial in allowing me to understand the intricacies of analyzing sequence and microbial data. Funding provided by the National Oceanic and Atmospheric Administration, Office of Education Educational Partnership Program award #NA16SEC4810009 and by the National Oceanic and Atmospheric Administration, Office of Education Educational Partnership Program with Minority Serving Institutions award (NA21SEC4810004). The contents of this work are solely the responsibility of the award recipient and do not necessarily represent the official views of the U.S. Department of Commerce, National Oceanic and Atmospheric Administration.

TABLE OF CONTENTS

Page

LIST OF TABLES

Page

LIST OF FIGURES

Page

CHAPTER I

INTRODUCTION

South Texas Banks and Flower Garden Banks

The continental shelf of the northwestern Gulf of Mexico (GoM) is a feature that supports diverse faunal communities and variations in environmental conditions. This continental shelf spans from the border of southern Texas to the easternmost region of Louisiana and is composed of primarily soft substrates, sand or clay sediments, that are interspersed with one of two uncommon topographic hard-bottom traits (Nash et al., 2013). These traits, salt diapirs and relict coral reefs and barrier islands, are present to the east and south of Matagorda Bay, respectively, as part of two geologically distinct reef systems along the Louisiana-Texas and South Texas Shelf, respectively (Rezak et al., 2015). Salt diapirs, or domes, provide bathymetrically high (shallow) hard structures that are formed from the intrusion of salt deposits, or rock composed primarily of sodium chloride, into the overlying soft substrate (Hudec and Jackson, 2007; Fuchs et al., 2011). In contrast, relict carbonate reefs are the unburied remnant hard substrate of the formerly-thriving shallow-water reefs that flourished until ~12,000 years ago when changes in temperature, sedimentation, and sea level led to their death (Belopolsky and Droxler, 1999; Pavliska, 2019). The South Texas Banks (STB), which are primarily deeper relict reefs in addition to shallower relict barrier islands, that lie to the south of Matagorda Bay, possesses a

persistent deep (~70 m) nepheloid layer both nearshore and offshore (Belopolsky and Droxler, 1999). In

contrast, the nepheloid layer is less persistent and generally present at deeper depths at the salt diapir banks. Nepheloid layers are water layers characterized by a significant amount of suspended sediment. The nearshore bottom nepheloid layer at the STBs is fed by runoff from coastal and inland water sources and is maintained by coastal wave action and currents (Shideler, 1981; Sahl et al., 1987). This nepheloid layer shows a seasonal fluctuation in distribution, being more restricted in the fall than in the spring, due to substantial water-column mixing in the fall season and may be found as shallow as 15 m (Shideler, 1981)(Hicks, Personal Observation). Tectonic forces and geological deposits elevate the relict reef structures above the seabed, allowing for diverse benthic organisms that inhabit these structures to persist both above and within the nepheloid layer (Rezak et al., 2015). Higher relief (i.e., taller) structures like the relict reefs allow for benthic organisms to avoid the otherwise antagonistic effect of consistent turbidity that results from the nepheloid layer.

To the east of Matagorda Bay lies the Flower Garden Banks (FGB) in the northwestern GoM off the coast of Texas and Louisiana. These banks were formed from uplifted salt diapirs, rising to within 17 m of the surface in some places (Hickerson et al., 2005). Like the STB, the FGB has a bottom boundary layer with a locally produced nepheloid layer that these salt diapirs provide relief from in varying degrees for coral forest communities (Bright et al., 1985). The FGB salt diapirs do provide greater relief from their nepheloid layer compared to the structures of the STB on average, thus providing more suitable habitat for benthic fauna. That said, despite the variability in nepheloid layer relief, presence, and thickness some benthic organisms are ubiquitous, revealing potential localized adaptations to turbid conditions (Bright and Rezak,

1977). Designated as a marine sanctuary by the National Oceanic and Atmospheric Administration (NOAA) in 1992 and expanded in 2021 to include 17 total banks, the Flower Garden Banks National Marine Sanctuary (FGBNMS) covers 160 square miles (414 km^2) (Register, 2021). Generally considered the healthiest coral reef system in the GoM the FGBNMS is characterized by stable or growing coral cover over the last 30 y to depths of 40 m (Johnston et al., 2021).

The benthic organisms, including octocorals, that occupy the hard bank structures of the FGB salt diapirs and STBs are primarily delimited by depth. Crustose coralline algae, filamentous algae, sponges, antipatharians, and octocorals are found above 50 m with approximately 21 species of shallow scleractinian coral persisting in the FGB, with very few shallow-water octocoral species being present (Hickerson et al., 2005; Hickerson et al., 2008; Rezak et al., 2015). At depths below 50 m the prevalence of crustose coralline and filamentous algae decreases while sponge, antipatharian and octocoral density increases (Bright and Rezak, 1977) with octocorals being abundant and diverse at depths below 43 m. These deeper abundant octocorals are found on the hard structures of both the FGB and STB, supporting diverse coral ecosystems at mesophotic depths in both regions.

Mesophotic Coral Ecosystems

These mesophotic coral ecosystems (MCEs) are coral, sponge, and algae dominated habitats that occupy a bathymetric, or depth, range from ~30 m to the maximum penetrative depth of sunlight that can support photosynthetic activity, usually around 150 m (Baldwin et al., 2018). The penetration of sunlight and therefore available photosynthetically active radiation into the water column can vary due to local conditions, such as turbidity. This light penetration explains the etymology of MCEs, with meso- meaning middle and -photic meaning light. The 30

m upper depth range of MCEs was defined by the limits of conventional scuba diving, as opposed to an ecologically informed categorization, though there is recent evidence supporting a rapid change in species turnover from shallow to mesophotic depths (Rocha et al., 2018). The change from shallow to mesophotic faunal communities, generally noted by a decrease in shallow specialists and increase in depth generalists, has even been observed in waters as shallow as 10 m, which are well above the 30 m threshold for MCEs (Laverick et al., 2017). Regardless, as the upper depth limit of MCEs is at the conventional scuba depth lower limit, MCEs are historically difficult to reach and are therefore understudied. With logistical limitations becoming less of a barrier due to the advent of technologies such as closed circuit rebreather diving, sonar and remote operated vehicles, the true breadth, range, and biodiversity of these cryptic ecosystems is becoming apparent (Bridge et al., 2013). General trends are being observed, such as a shift from predominantly zooxanthellate corals (e.g., Scleractinia) to azooxanthellate coral species, primarily represented by Octocorallia and Antipatharia (Roberts et al., 2006).

With a growing understanding of MCEs, information about the coral species that compose them is being revealed, including that coral species that make up MCEs are not confined to mesophotic depths. It is now understood that many of the coral species found in MCEs are found in depths both above and below the general 30–150 m depth range used to define MCEs, with many shallow-water species being found at or above mesophotic depths (Blyth-Skyrme et al., 2013). This greater appreciation for bathymetric overlap in species' distributions has led to the refuge hypothesis, which suggests that shallow-water species may find refuge from anthropogenic perturbations at deeper depths, especially in the upper mesophotic zone (> 60 m; (Slattery et al., 2011)). These protected conspecifics would then be

able to reseed the shallow reefs when favorable conditions return. Some studies suggest that the refuge hypothesis may not hold true as most coral species have a strongly defined depth preference despite occasionally being found outside of that range (Rocha et al., 2018). In the case that the refuge hypothesis is true, MCEs provide refuge for shallow-water species. In the case that it does not, MCEs are highly unique habitats home to depth-restricted coral and sponge species. Regardless, many coral and sponge species provide an ecosystem service for MCEs as foundational species that form a highly structured three-dimensional habitat that is home to many commercially important fish species, such as red snapper in the STB (Bright and Rezak, 1977). As these MCE habitats are highly productive, an examination into their connectivity is also necessary to better understand the robustness of the system of reefs as a whole.

The larva of coral at shallow to mesophotic (~15-60 m) FGB reefs are carried by Loop Current Eddies (LCEs) leading to a high degree of local settlement (Limer et al., 2020). Larval retention combined with geographical isolation from other major reefs, the nearest being Campeche Bank off Mexico's Yucatan Peninsula nearly 700 km away, means that the reefs of the FGB are unique in their coral communities (Hickerson et al., 2008). It has been argued that these same LCEs provide pathways of connectivity between isolated deep mesophotic and deep-sea ecosystems, such as the FGB and STB, however long term variations in shedding of eddies complicates the prediction of the degree of connectivity present (Ritchie et al., 2008). Thus, these reefs may experience periods of isolation and high local settlement. The potential lack of connectedness between reefs also brings to question their isolation from anthropogenic perturbations.

Despite their general distance from shore and depth, MCEs are vulnerable to anthropogenic disruptions such as pollution, invasive species, and oil production activities

(White et al., 2012; Rocha et al., 2018). The 2010 Deepwater Horizon oil spill in the GoM exemplifies the impact that human activity can have on these habitats in this region. Assessments looking into the damage caused by this single, but significant, event have shown that adjacent to the Macondo well up to half of large octocorals had suffered injury from oil exposure (Etnoyer et al., 2016). Through the proper management of MCEs, adjacent MCEs, fisheries, and shallow-water reefs could be protected as was done to effect in 1999 when a permanent deep-water fisheries ban was put into place in the US Virgin Islands that resulted in the recovery of red hind grouper stocks in nearby shallow reefs (Richard, 2005).

For such efforts, assessments of these communities and their health as well as an understanding of the factors governing these patterns are essential. While conditions may differ among the banks it is generally observed that there are high growth densities of ahermatypic coral species on these western GoM MCEs. In these deeper habitats, corals, including those in subclass Octocorallia, serve as keystone species by providing complex structural lattices that are occupied by invertebrates, benthic organisms, and juvenile and adult fish (Bongiorni et al., 2010; Baillon et al., 2012; Blyth-Skyrme et al., 2013). Octocorallia, a subclass of corals whose polyps have eight-fold symmetry, are a diverse and understudied group of organisms that comprise the majority of classified coral species and that are found primarily below 50 m (Cairns, 2007). In the GoM they can comprise a significant proportion of coral species on MCEs (Rodriguez et al., 2018). Because octocorals are foundational organisms at mesophotic depths in this region, a low cost and simple metric for assessing the health of octocorals is needed. Microbiomes may serve as this health metric for octocorals.

Microbiomes

A microbiome consists of the microorganisms that live in and on a habitat, in this case a coral organism (Marchesi and Ravel, 2015). Although the microbiome of shallow-water corals generally includes symbiotic algae, known as zooxanthellae, which provide sufficient energy for host metabolism through photosynthesis (LaJeunesse, 2020), corals on MCEs tend not to host these microbial algae due to limited availability of light. The bulk of research on coral microbiomes and their drivers has focused on these shallow-water and primarily scleractinian coral's relationship with zooxanthellae, especially in regard to the process of zooxanthellae expulsion known as coral bleaching. More recently, a greater appreciation for other microbes, including fungi, viruses, bacteria, archaea, and dinoflagellates (van Oppen and Blackall, 2019) that make up the microbiomes of corals is growing. The important roles that these other microbes play in coral holobiont health are starting to become understood. For example, bacteria and archaea are now known to play roles in nutrient cycling, immunity, and reproductive success for a variety of coral host species (McDevitt-Irwin et al., 2017). In studies of bacterial and archaeal constituents of shallow-water (~17 m) octocoral microbiomes, metagenomic sequencing has revealed a suite of abiotic stress response, nutrient acquisition and antiviral defense (CRISPR-Cas9, endonucleases) genes (Keller-Costa et al., 2021). In addition, microbial constituents have been postulated as the main source of nitrogen for corals that unexpectedly flourish in oligotrophic conditions where nitrogen should be a limiting growth factor, exemplifying their importance to coral reef ecosystem function (Sammarco et al., 1999; Rädecker et al., 2015).

In response to disturbance, the healthy microbial consortium of microbes can change, a process called dysbiosis, leading to disease states in the coral host. This change in microbiome composition has been observed in octocorals in the Mediterranean at mesophotic depths in

response to marine heatwaves prior to any visible necrosis in octocoral tissue (Corinaldesi et al., 2022). Dysbiosis has been suggested to even play a role in coral epidemics, such as Stony Coral Tissue Loss Disease (Neely et al., 2020). This and other work suggest that microbiomes can be causative and indicative of coral health. To understand when an unhealthy state is reached, and which microbes can serve as a tool for intervention, a fundamental understanding of a healthy baseline microbiome's composition and its drivers is needed.

The task of determining microbiome composition is complicated by the fact that the composition of the microbiome can be driven by a myriad of factors, including geographical distribution, season, environmental factors, and evolutionary history. Geographical distance was found to increase dissimilarity in scleractinian coral microbiomes, while Caribbean octocoral *Erythropodium caribaeorum* had a conserved core microbiome with some variations in microbial taxa across distance (McCauley et al., 2016; Dunphy et al., 2019). Seasonality between summer and winter has been found to be an explanatory factor in microbiome community patterns in octocorals in tropical and temperate Australia and the Caribbean (McCauley et al., 2020; Haydon et al., 2022). Environmental factors, such as depth, and a coral species' status as a depth generalist or depth specialist across shallow to mesophotic depths have been linked to changes in microbiome community as well (Glasl et al., 2017).

Phylosymbiosis has been demonstrated as a major driving force for microbiome composition in scleractinian corals, even when compared to environmental drivers (Pollock et al., 2018). The correlation of microbiome composition and host phylogeny has also been seen in octocorals from off the coast of Portugal (Keller-Costa et al., 2021). In the phenomenon known as phylosymbiosis, more closely related host species have more closely related microbial constituents (Lim and Bordenstein, 2020). The importance of phylosymbiosis is further

underpinned by work showing that in some cases coral microbiomes within a single coral species were stable across a variety of abiotic conditions and geographic locations (Bourne et al., 2016). It is therefore likely necessary to analyze species of coral individually when looking to establish baseline microbiomes.

Sequencing Depth Effect

Microbiome profiling utilizing whole genome, metagenome, and marker gene sequencing has been empowered by the dropping cost of high-throughput sequencing and bioinformatic analyses (Fraher et al., 2012). Despite the clear utility of these techniques and the importance of microbiome characterization, there is a lack of consistency in the parameters surrounding handling of samples, sequencing, and downstream analysis for sequencing based microbiome research. The duration of cold storage and the solution that samples are kept in prior to processing has a meaningful effect on microbiome community profiling (Chen et al., 2019). Primer bias, where certain primers targeting the *16S* ribosomal RNA (rRNA) gene differentially amplify one bacteria's template over another, is a poorly understood yet present confounder in microbiome analysis (Silverman et al., 2021). The reference database used also can lead to significant differences in detected amplicon sequence variants (ASVs) and beta diversity of microbiome samples (Ramakodi, 2022). In short, confounding elements can be introduced at every step of microbiome analysis, and there is merit in investigating each of these steps thoroughly.

The effect of sequencing depth on the characterization and trends associated with microbiomes when using *16S* rRNA sequencing is one such factor. Sequencing depth can be understood as the amount of reads (read = small fragment of amplified DNA from the target region) per sample, with a greater number of reads equating to a greater sequencing depth

(Gweon et al., 2019; Jiang et al., 2019). In one study on fecal bacteria samples microbiome richness did not differ between three different sequence depths at the phylum or class level, nor did the alpha diversities of the microbiomes (Zaheer et al., 2018). Other studies detected more bacterial taxa with greater depth, but also found that diversity trends for the microbiome samples were consistent regardless of depth (Jovel et al., 2016). If the purpose of your microbiome sequencing is to identify rare taxa, then further sequencing depth seems beneficial, but to determine trends such as alpha diversity a lower depth appears to be sufficient (Lundin et al., 2012). Regardless, further investigation of the effects of sequencing depth on microbiome profiling is needed, especially in non-human and other well documented sample types.

Purpose

In the western and northwestern GoM, an assessment of mesophotic octocoral microbiomes has not yet been conducted despite numerous species being injured by the Deepwater Horizon Oil Spill and these species being under threat from anthropogenic activity in this region, including mining and oil activity, pollution, and disease (Gil-Agudelo et al., 2020). Therefore, this thesis will provide the first assessment of the microbiomes of 13 octocoral groups from western GoM MCEs. Not only is there an opportunity to utilize microbiomes as a low-cost and efficient method for understanding host health in this region, as has been previously done in agricultural and medical applications (Wilmanski et al., 2021; Wilhelm et al., 2022), this work can also allow for proactive conservation applications. Once beneficial immune microbes have been identified, probiotics can be applied in corals to arrest disease (Peixoto et al., 2021) or bleaching (Rosado et al., 2019). Sequencing microbial communities of octocoral samples from the western and northwestern GoM MCEs at low and high sequence depths for this thesis will open the door for improved management, remediation, and conservation practices for these

understudied organisms and the ecosystems they constitute while refining the methodologies used to study them.

Objectives

My objectives for this research are:

1. To provide a preliminary characterization of the bacterial and archaeal taxa of the microbiomes of mesophotic octocoral species found along the western GoM.
2. To determine extent of phylosymbiosis, reef type, spatiotemporal factors, and depth in driving microbiome composition.
3. To illuminate the effect sequence depth has on microbiome profiles from octocoral samples.

Hypotheses

My hypotheses are:

1. Octocoral species microbiomes will share the same predominant microbial taxa.
2. Microbiome community composition is expected to primarily be driven by octocoral group differences as opposed to spatiotemporal and other factors.
3. Low sequence depth will sufficiently capture microbiome trends and diversity metrics.

CHAPTER II

METHODS

Sample Collection

Octocoral samples (n = 98, Table 1) were collected from natural and artificial reefs primarily by remotely operated vehicle (ROV; University of North Carolina at Wilmington *Super Phantom* ROV, Schmidt Ocean Institute *SAAB SeaEye Falcon* ROV, and the FGBNMS Foundation *Mohawk* ROV) and scuba between 2004 and 2021 at ~30–150 m (Table 1) and were provided by Dr. David Hicks and FGBNMS subsample collection for the purpose of this project. Collection seasons were classified as either Fall (September, October, November) or Summer (June, July, August). Collection sites were located from the southern tip of Texas, off the coast of Brownsville, to the FGBNMS, off the coast of Galveston, and extending east to the Florida panhandle (Figure 1). Once brought to the surface, tissue samples were sorted and given a preliminary octocoral species identification and collection identification code. Afterwards octocoral tissue samples were preserved in 100% ethanol and stored at -20°C for further processing onshore. A subset of samples (n = 10) was also provided by the Smithsonian Institution National Museum of Natural History (USNM) collection with sample information ascertained from the USNM Department of Invertebrate Zoology Collections database (https://collections.nmnh.si.edu/search/iz/).

16S rRNA Sequencing

DNA was isolated with a DNeasy Blood & Tissue Kit (#69506, QIAGEN, Hilden Germany) from a ~0.3–0.5 cm segment of polyp-containing tissue for each of the 98 octocoral samples following the manufacturer's protocol with the following modifications: 3 µl of RNase A was added (#EN0531, ThermoFisher Scientific, Waltham, Massachusetts) during the initial lysis step and final purified DNA was eluted in 50 µl of molecular biology grade water. Isolated DNA was then stored at -20℃ until amplified using polymerase chain reaction (PCR) with Earth Microbiome Project (EMP) primers 515F (5'-GTGYCAGCMGCCGCGGTAA; Parada et al., 2016) and 806R (5'-GGACTACNVGGGTWTCTAAT; Apprill et al., 2015) that target the hypervariable V4 region of the *16S* rRNA gene. The 25 µl PCR reaction contained 12.5 µl (1X) AmpliTaq Gold 360 Master Mix (#4398881, Applied Biosystems, Waltham, Massachusetts), 1.0 µl of DNA template (1.2–2 ng μl^{-1}), 0.5 µl 515F primer (0.2 µM) and 0.5 µl 806R primer(0.2 µM), and remaining volume of UV-sterilized molecular biology grade water and was run on a Mastercycler X50s thermal cycler (Eppendorf, Hamburg, Germany) using the following protocol: initial denaturation for 10 min at 95℃, 32 cycles of 95℃ denaturation for 45 s, 50℃ annealing for 60 s, and 72℃ extension for 90 s, followed by a 10 min final extension at 72℃ before dropping to 4℃ for temporary holding before visualization. PCR products were visualized via gel electrophoresis by running on 3–5% agarose gel (#BP2410, ThermoFisher Scientific, Waltham, Massachusetts) for 30 min at 110 V in 1X TAE (Tris-acetate-EDTA) buffer (pH 8.3) (#1.06023, Sigma-Aldrich, St. Louis, MO) to confirm successful amplification with EMP primers. For successful amplicons, DNA concentrations were quantified and normalized to 1–5 ng μl^{-1} using a Qubit Flex Fluorometer (#Q33327, ThermoFisher Scientific) system using molecular biology grade water. Normalized DNA extract samples were then loaded onto a 96

well plate in 20 µl volumes and shipped to the University of Michigan Microbiome Core (University of Michigan, Ann Arbor, Michigan, https://microbe.med.umich.edu/welcome-university-michigan%E2%80%99s-microbiome-core) for High-Depth *16S* EMP Library Generation (~50,000 sequences per sample), normalization, and QC. Library generation was done by the University of Michigan Microbiome Core utilizing the dual indexing sequencing strategy modified with EMP primers using Illumina sequencing on the MiSeq system (Illumina, San Diego, California; Kozich et al., 2013, Walters, 2016). A subset of samples (n = 25) from five octocoral groups were run ahead of the full (n = 98) sample set to confirm the efficacy of this protocol at generating usable microbiome sequence reads using the protocol above and to differentiate the effect of sequence depth on microbiome characterization and analysis outcomes. This preliminary low-read run was performed on the more cost-effective Low-Depth *16S* EMP Library Generation (~10,000 sequences per sample) from the University of Michigan Microbiome Core. The 25 preliminary samples were *Thesea nivea* (n = 5), *Leptogorgia virgulata* (n = 5), *Paracis* cf. *enopla clade 1* (n = 5), *Scleracis sp.* (Red) (n = 5), *Scleracis sp.* (Yellow) (n = 5). *Scleracis sp.* (Yellow) and (Red) were kept separate as there is data indicating they may belong to different unreported species (Easton, unpublished data).

Data Analyses

Octocorals were split into thirteen groups, primarily by genera: *Placogorgia, Bebryce, Thesea, Scleracis, Muricea, Swiftia, Paramuricea/Placogorgia, Nicella, Callogorgia, Leptogorgia, Ellisella, Paracis,* and *Thesea nivea*. *Thesea nivea* was separated from other *Thesea* spp. because it likely belongs to a different family from other *Thesea* (McFadden et al., 2022). Within each sample information related to sampling location (bank and reef), reef type (natural versus artificial), sampling season (fall versus summer), region (FGB versus STB), and depth (in

meters) was collected as best as possible with some gaps due to historical record keeping errors (Table 2). Some samples from the USNM collection were omitted from region analysis as some were from SW or NE GoM. Raw sequence reads were imported into the next-generation microbiome bioinformatics platform Quantitative Insights Into Microbial Ecology or QIIME2 version 2021.8 (Caporaso et al., 2010) (Appendix B). In QIIME2, installed on Texas Advanced Computing Center (University of Texas at Austin, Austin, Texas), raw sequence files were filtered or denoised based on quality and compared to the SILVA version 132 database (Quast et al., 2013), which contains quality-controlled aligned *16S* rRNA gene sequences, for classification. The denoising involved removing sequences shorter than 200 bp, incorrectly joined or chimera sequences (see Appendix B) and reads with maximum expected error higher than 2. Amplicon sequence variants (ASVs), which are the individual DNA sequences of the *16S* rRNA gene that differ by one or more nucleotides, were then organized across individual samples using DADA2 from the filtered base pairs (Callahan et al., 2016). The ASVs were referenced against the SILVA database 132 using the classify-consensus-vsearch method in QIIME2, allowing for the assignment of taxonomic rank of ASVs.

The QIIME2 classification, ASV, and metadata outputs were then merged into a PhyloSeq object using the R package "PhyloSeq" (McMurdie and Holmes, 2015) (Appendix B). The high-quality and referenced sequences organized in the PhyloSeq object were then analyzed to assess and visualize microbial diversity and abundance (Objective 1) and influencing factors (Objective 2). For the full 98 sample set all samples were first rarified to 7621 to eliminate sampling effort bias (Figure 2). For the high versus low sequence datasets (Objective 3), they were rarified to the highest possible amount of reads for each data set, 10,326 for the high reads and 2898 for the low reads (Figure 3A-B).

The number of bacterial and archaeal taxa within the microbiome of each sample, or alpha diversity, was determined using observed, Chao1, and Shannon indices and compared across octocoral groups to assist in characterizing microbiome prokaryotic diversity differences (Shannon, 1948; Chao, 1984) (Hypothesis I, III). The package "microbiome" with the microbiome::alpha function was used to elucidate these alpha diversity measurements, with the plot_richness function from "Phyloseq" used for visualization (Lahti et al., 2017). As Shannon index alpha diversity values were not normally distributed, a Kruskal Wallis H test was preformed to determine significant differences between octocoral groups and a pairwise Wilcoxon rank sum test was performed to determine which groups harbored the greatest differences with Benjamini-Hochberg adjusted p-values using the kruskal.test and pairwise.wilcox.test functions in R (Hollander et al., 2013). The visualized differences in microbiome alpha-diversity revealed which species harbor more diverse microbiomes and whether the core microbial species of the microbiomes are shared between octocoral species (Hypothesis 1).

To determine the driving forces behind microbiome composition a permutational analysis of variance (PERMANOVA) (Anderson, 2014) was performed to determine drivers and differences in microbial communities of octocorals by reef type, octocoral group, seasonality, region, and depth (Hypothesis 2). The PERMANOVA was run using the adonis2 function in R from the "Vegan" package on Bray Curtis distances with standard 999 permutations and ordered by terms (Oksanen et al., 2007). Nonmetric multidimensional scaling (nMDS) was then used to visualize the drivers of microbiome composition, for example which has the greater effect between octocoral group and reef type (Kruskal, 1964) (Hypothesis 2). The nMDS was calculated using the ordinate function on Bray Curtis distances and visualized with

plot_ordination from the package “Phyloseq”. The same alpha diversity analysis and nMDS visualizations were performed on the subset high and low sequence depth datasets to determine the effect of sequencing depth on microbiome characterization outcomes (Hypothesis 3).

CHAPTER III

RESULTS

Sequence Coverage

All 98 (100%) octocoral samples successfully returned usable sequence data for the high-read run and 24 out of 25 (96%) returned usable sequence data for the low-read run; one *Paracis* cf. *enopla clade* 1 sample did not successfully run for the low read set leaving *Paracis* cf. *enopla clade* 1 at an n of 4 for analysis. Sequence depth for the high-read run ranged from 7621 to 159,321; rarefication to 7621 was sufficient to reach rarefaction curve asymptotes for all samples (Figure 2)(Figure 4A-B). Of the 98 samples, 91 out (93%) returned a sequence depth of between 7621 and 60,000 reads and 7 (7%) samples returned sequence depth of over 100,000 reads

(Figure 4A-B). Sequence depth for the low-read dataset ranged from 2898 to 11,501; rarifying to remove sampling effort bias sufficiently reached rarefaction curve asymptotes for these samples (Figure 3B).

Hypothesis 1 & 2: Microbiome Community Composition and Trends

The majority of the sequenced microbial taxa was only found in 1 or 2 octocoral samples indicating a high level of rare or unique taxa (Figure 5). Following filtering for chloroplasts, mitochondria, and unassigned taxa and subsequent rarefaction, 1542 ASVs were identified for the low-read dataset and 14,119 were identified for the high-read dataset. The average Shannon

index alpha diversity was low (1.288–3.225) for each octocoral group except for *Thesea nivea* and *Bebryce,* which had alpha diversities of 5.166 and 5.616, respectively (Table 3, Figure 6A). The observed and Chao1 alpha diversity values also followed this pattern with low alpha diversity for all groups apart from *Thesea nivea* and *Bebryce* (Figure 6B). A Kruskal Wallis H Test on Shannon index values for all 13 octocoral groups returned a p-value equal to 2.601e-07, signifying significant differences were present between octocoral groups (Hypothesis 1 and 2). A pairwise Wilcoxon rank sum test revealed *Bebryce* and *Thesea nivea* harbored significant differences in alpha diversity compared to other octocoral group microbiomes (Table 4).

The main driver of clustering based on Bray Curtis similarity nMDS plots of microbial composition was octocoral group, as can be seen with the tight clustering of octocorals *Muricea, Thesea nivea, Bebryce, Scleracis, and Leptogorgia* (Figure 7). This importance of octocoral group was also supported by an nMDS and PERMANOVA (Table 5) (Figures 8-11), which showed octocoral group explained the greatest variation in microbiome composition ($p = 0.001$, $R2 = 0.492$) followed by reef type ($p = 0.001$, $R2 = 0.053$), region ($p = 0.001$, $R2 = 0.045$), season ($p = 0.001$, $R2 = 0.031$), and depth ($p = 0.001$, $R2 = 0.029$).

Specific examination of the microbial taxa present was done by merging samples' microbiomes to class level by octocoral group in a bar plot (Figure 12A-B). As mentioned previously with alpha diversity being higher, the number of microbial classes present in the bar plots of *Thesea nivea* and *Bebryce* was the greatest of all octocoral groups. The microbiomes of each octocoral group were generally dominated by a few key microbial classes shared between all thirteen octocoral groups (Table 6). The five most predominant microbial class were Gammaproteobacteria, Nitrososphaeria, Mollicutes, Spirochaetia, and Alphaproteobacteria. Gammaproteobacteria were found to be the predominant microbial class in 12 out of the 13

octocoral groups, composing between 29.9% to 77.9% of the microbial taxa. Nitrososphaeria ranged from 11.8% to 43.8% and was the second and third most abundant class in 4 and 3 of the 13 octocoral groups, respectively. Mollicutes ranged from 10.7% to 40.3% of microbial taxa and was the most abundant in *Thesea*, second most in 4, and third most in 1 octocoral group. Spirochaetia composed 27.1% of *Muricea*'s microbiome and was not in the top 3 class for any other octocoral group. Alphaproteobacteria ranged from 2.9% to 19.5% and was the second and third most abundant class in 2 and 4 of the 13 octocoral groups, respectively. Other abundant microbial classes included Clostridia (second most abundant in *Placogorgia,* 19.5%,), Bacteroida (third most abundant in *Bebryce* and *Thesea nivea*, 8.9% and 9.0%), Fibrobacteria (third most abundant in *Callogorgia*, 7.9%), Nitrospira (third most abundant in *Nicella*, 4.2%), and Bacilli (third most abundant in *Ellisella* 2.4%).

To gain a better understanding of the potential roles microbes may be playing within the microbiomes, the six most prevalent microbial genera were visualized and examined for each octocoral group (Figure 13A-C). The top three most prevalent microbial genera were reported in Table 6 as they comprised 26.1% to 91.7% of the total microbial genera present in each octocoral group. Generally, the microbiomes were dominated by *Endozoicomonas, Mycoplasma,* Candidatus *Nitrosopumilus,* BD1-7 clade (of the family Spongiibacteraceae), and *Spirochaeta*. *Endozoicomonas* was one of the two most abundant microbial genera in 11 out of 13 octocoral groups, composing between 10.2% to 57.9% of the microbiome community. *Candidatus* Nitrosopumilus was one of the three most abundant microbial genera in 9 out of 13 octocoral groups, composing between 5.6% and 45.5% of the microbiome community. *Mycoplasma* was one of the three most abundant microbial genera in fewer octocoral groups, 6 out of 13 octocoral groups, but contributed higher percentages in microbiomes it was found in at a range of 12.4% to

41.7%. BD1-7 clade (12.9–46.8%, 3 groups), *Spirochaeta* 2 (5.8–30.9%, 3 groups), *Thiohalophilus* (8.8-11.8%, 3 groups), *Alteromonas* (26.2%, 1 group), uncultured microbial taxa (9.6%, 1 group), *Nitrospira* (4.8%, 1 group), and *Spiroplasma* (2.1%, 1 group) all appeared in the three most abundant microbial genera as well.

Hypothesis 3: High versus Low Read Sequence Differences

The alpha diversity values for the high-read dataset were higher than the low-read dataset for observed, Chao1, and Shannon indices (e.g., Shannon index alpha diversity: *Thesea nivea* low 4.616 vs *Thesea nivea* high 5.174), however the trends are the same between both datasets as follows (Table 7, Figure 14A-B). For both the low- and high-read set, four of the five octocoral species had low alpha diversity for all three indices, with *Thesea nivea* having a significantly more diverse microbiome compared to the other four species tested (Table 7). A Kruskal Wallis H Test on Shannon index derived alpha diversity values revealed significant differences between octocoral groups for the high-read (p-value = 0.0078) and the low-read datasets (p-value = 0.0152). A pairwise Wilcoxon rank sum test revealed *Thesea nivea* harbored significantly different alpha diversity compared to the four other octocoral group microbiomes, for both high- and low-read groups (Table 8, Table 9). The nMDS plots show that the low- and high-read datasets had similar clustering patterns with all samples clustering by species, and notably *Scleracis sp.* (Red) and *Scleracis sp*. (Yellow) clustered together for both datasets (Figure 15A-B). The top six bacterial and archaeal classes for the high and low reads were the same for all species, however they differed in their distribution and abundance amongst the different octocoral species (Figure 16A-B). For example, in the low-read dataset the microbiome of *Leptogorgia virgulata* was predominated by the bacterial class Spirochaetia (~10,500 reads), but

in the high-read dataset *Leptogorgia virgulata* had few reads for Spirochaetia (~100 reads) (Figure 12B).

CHAPTER IV

DISCUSSION

Hypothesis 1 & 2: Microbiome Community Composition and Trends

Octocorals are organisms that often comprise much of the coral community on mesophotic coral ecosystems in the western GoM and importantly to this project are understudied in this region. To improve our understanding of these foundational organisms and to improve their conservation outcomes, approaches such as microbiome characterization are needed. It is well established that the microbiomes of organisms have been shown to play a role in host fitness and to change in response to stressors, and this importance of microbiome health to host fitness extends to foundational and threatened species as well (Bahrndorff et al., 2016; West et al., 2019). By understanding the healthy microbiome composition of an organism it is possible to monitor its health, to understand how it is responding to stressors, and to provide beneficial microbes to alleviate the effects of stressors as has previously been done with coral bleaching (Rosado et al., 2019).

This study provided preliminary data on the trends and composition of mesophotic octocoral microbiomes from the western GoM. The microbiomes characterized from 13 mesophotic octocoral groups in this study were generally low in alpha diversity and predominated by a few primary taxa. In contrast, high alpha diversity was observed for two of

my octocoral groups, *Bebryce* and *Thesea nivea*, and this result was found to be consistent across high- and low-read sequence runs. The low alpha diversity observed in this study's octocorals are a well-examined characteristic of octocoral microbiomes and can be primarily explained by the fact that octocoral microbiomes are generally composed of a few core microbial taxa making up a large proportion of the microbiome (Bayer et al., 2013; Correa et al., 2013; van de Water et al., 2017), as was seen in this study.

The predominance of specific microbial taxa in coral microbiomes is unsurprising. Corals, including octocorals, have largely been shown to have very distinct microbiomes from surrounding seawater (Hadaidi et al., 2017). This distinctness may be due to how corals regulate their microbiomes. For example, using biological control or predatory microbes that prevent the invasion of other taxa has been observed in scleractinian (subclass Hexacorallia) corals belonging to the genus *Porites* (Welsh et al., 2016). Octocorals also produce antimicrobial compounds in their tissue, potentially as a means of excluding certain microbial taxa from entering from the surrounding water as a part of the coral immune system (Harder et al., 2003). Similar compounds have been isolated from octocoral-derived microbes, showing that once established, the microbiome may support in maintaining the compositional status quo (Zheng et al., 2015). Lastly, octocorals also produce compounds involved in quorum-sensing, which is a molecule based form of communication between microbial organisms (Hunt et al., 2012). By interfering with microbial communication, octocorals have the capacity to stimulate or inhibit the growth of targeted taxa within their microbiomes. It can therefore be inferred that the octocorals in this study were similarly regulating their own microbiomes to some degree based on the shared predominance of specific microbial groups, such as Gammaproteobacteria, Nitrososphaeria, Mollicutes, Spirochaetia, and Alphaproteobacteria.

It is important to note that this low octocoral microbiome diversity is a general rule with known exceptions of documented cases of some octocoral species demonstrating higher microbiome alpha diversity. For example, a recent study comparing two temperate octocoral species and two tropical octocoral species collected from the same respective sites revealed one temperate and tropical octocoral possessed high alpha diversity, while the other tropical and temperate species had low alpha diversity (Haydon et al., 2022). Octocoral microbiome alpha diversity of coral colonies has also been observed to increase in response to stressors as opportunistic, rare, and pathogenic bacteria invade the host tissue when the host loses the capacity to regulate its microbiome (Corinaldesi et al., 2022). However, this stressor-induced increase in alpha diversity is likely not the reason for *Thesea nivea*'s or *Bebryce*'s high alpha diversity because the microbial taxa observed in their microbiomes are associated with healthy coral colonies and all colonies had higher diversity regardless of collection location and time. Although it is unclear from this study the exact mechanisms through which these octocorals are regulating their microbiomes, it is clear that it is occurring as there is shared low alpha diversity and predominant beneficial microbial taxa with congenerics demonstrating regulated and distinct microbiomes consistent with literature (van de Water et al., 2018).

It is also noteworthy that microbiomes in this study are driven primarily by the octocoral groups themselves as indicated by clustering in nMDS and PERMANOVA, which revealed octocoral group as the leading factor to describe microbiome structure. Although it has been observed that spatiotemporal and other factors may influence the microbiome composition of corals in southeast Asia (Deignan et al., 2023), little variation was observed in microbiomes of octocorals across space and time in the Mediterranean (van de Water et al., 2017; van de Water et al., 2018). In the western GoM, the persistent nepheloid layer in addition to the main

dynamical feature of the loop current (Hamilton et al., 1999) may also serve as factors that shape microbiome composition in this region and may play important roles in variation in microbiome stability depending on the site, type of coral, and other factors. For these western GoM octocorals, depth, region, season, and reef type all played a significant but lesser role in microbiome composition compared to octocoral group, potentially signaling phylosymbiosis is at play and that further study is needed to understand the effect of the other factors on microbiome stability.

Evidence of phylosymbiosis in octocorals has been documented with symbionts belonging to the *Hahellacae* family of Gammaproteobacteria having phylogenetic trees that corresponded to the systemic classification of their host octocoral species, indicating coevolution (La Rivière et al., 2013). In scleractinian corals phylosymbiosis has been found to be occurring throughout their entire phylogenetic history; interestingly, this pattern was specific to the part of the coral tested, with the mucus microbes not demonstrating this cophylogeny as opposed to the skeletal and tissue microbes that did (Pollock et al., 2018). As most of the research into coral microbiome drivers has come from scleractinian corals as opposed to octocorals, the data from this thesis on what may be driving octocoral microbiome composition fills an important gap in knowledge. While this study only goes as far as nMDS clustering and PERMANOVA to determine microbiome drivers and does not examine microbiomes by specific coral parts (e.g., mucus vs skeletal), it does show that octocoral group is the primary driver, similar to other corals shown to have phylosymbiotic coevolution of host and symbiont taxa. The reason for these microbial taxa to be selected for, and stable through evolutionary time, is that they may be providing some fitness benefit for the host organism as obligate associates.

The functions of the different core microbiome constituents in this study are still largely unknown, but the predominant microbial constituents identified in this study are typically associated with healthy corals and are predicted to play roles in nutrient cycling, immune function, and microbiome regulation. *Endozoicomonas* is a regularly found major component of microbiomes in Caribbean, Mediterranean, and cold-water octocorals (Ransome et al., 2014; Robertson et al., 2016; van de Water et al., 2018). Similarly, in this study *Endozoicomonas* was found to be a core member of every octocoral group's microbiome (Figure 8A-C) (Table 10). While the function *Endozoicomonas* serve as a member of microbiomes is an area of active investigation, this genus is postulated as being involved in nutrient cycling and acquisition and in microbial community regulation (Neave et al., 2016). Like *Endozoicomonas, Mycoplasma* is commonly found to be predominant taxa in octocorals from both warm- and cold-water environments (Kellogg et al., 2009; Gray et al., 2011). *Mycoplasma* is generally considered a parasitic bacterial genus, and while *Mycloplasma* function in coral microbiomes has yet to be determined, prevalence in both scleractinian and octocoral species of coral indicates it may be serving a distinct and beneficial role. *Spirochaeta* is similarly cryptic in function as a member of coral microbiomes but free-living species have been confirmed to have the capacity for nitrogen and carbon fixation (Lilburn et al., 2001). Whole-genome sequence analysis on the archaea genus *Nitrosopumilus* has shown that they are ammonia-oxidizing autotrophs and are therefore potentially serving a role in the nitrogen cycle for their coral hosts (Siboni et al., 2008; Bayer et al., 2016). *Spirochaeta* and *Nitrosopumilus* both exhibit species capable of performing portions of the nitrogen cycle and therefore may be serving that role for this study's octocorals. In short, the microbial taxa found composing the core of the study's octocorals are consistent with healthy

microbiomes of those seen in octocorals sampled globally and may be serving roles in immune and metabolic functions for their hosts.

Apart from the microbiome constituents themselves indicating healthy microbiomes the primary sample sites, the STB and FGB, are both arguably healthy coral habitat. The STB octocorals in this study were sampled at mesophotic depths, which has been shown to provide a partial buffer against some anthropogenic stressors at other locations (Smith et al., 2016). Many of the FGB samples, while also being sampled at mesophotic depths, come from a protected marine sanctuary that has existed since 1992 and contains a mean coral cover greater than 50% (Johnston et al., 2016). Both the STB and FGB regions have seen limited impact of coral disease and invasive species, such as the red lionfish (*Pterois volitans*), which has only been observed in FGBNMS since 2011 with little impact on biodiversity thus far (Johnston et al., 2021; Blakeway et al., 2022; Johnston et al., 2023). As this studies' corals were collected by researchers aiming for healthy samples, and they were collected from primarily healthy habitats, these microbiomes likely represent healthy baselines for these octocoral groups. However, the octocoral group *Bebryce* did show a potentially pathogenic microbe, from the genus *Vibrio,* as a major constituent of its microbiome. Pathogenic *Vibrio* have been shown to be involved in disease-induced bleaching, and white and black band diseases in multiple coral species (Sussman et al., 2008; Arotsker et al., 2009; Mills et al., 2013). Further examination of *Bebryce* species' microbiomes could be done by sampling for both visibly healthy and unhealthy samples to confirm *Bebryce*'s healthy baseline composition.

Because the octocoral samples collected in this study were not collected for the purpose of this project, several limitations regarding the study should be addressed. The octocoral samples were collected for, in part, taxonomic examination, meaning that they were selected

partially due to their outwardly healthy appearance. The collection of outwardly unhealthy octocoral samples, or samples taken from proximity to anthropogenic disturbances, would have likely allowed for the examination of dysbiosis and confirmed that the microbiomes in this study represent healthy microbiomes. That said, this limitation can be largely ignored as the constituents of the microbiomes presented here match other studies' observations of healthy octocoral microbiomes (van de Water et al., 2018). Another limitation is that when sampled, not all octocoral samples had depth measurements or month sampled recorded, reducing the analyses that could be done to examine the effect of abiotic factors on microbiome composition to some degree. In addition, many octocoral genera were sampled strictly from one reef type, region, or season, further reducing the ability to examine how these three factors may be playing a role separate from octocoral group. Lastly, this study is limited in that it utilized *16S* rRNA sequencing as opposed to other more comprehensive sequencing techniques like shotgun metagenomic sequencing. Unlike *16S*, which is limited to examining a single marker gene found in bacteria and archaea, metagenomic sequencing allows for the examination of all microbes and their functional genes (Zinicola et al., 2015). When compared directly, *16S* rRNA sequencing is less comprehensive in its ability to identify microbial taxa, especially less abundant taxa (Durazzi et al., 2021). Future studies could build upon the work of this thesis by expanding and targeting sampling for further analysis of microbiome drivers and utilizing other sequencing methodologies to compare with the data from this project.

Hypothesis 3: High versus Low Read Sequence Differences

16S rRNA sequencing has allowed for the rapid identification of microbial taxa for the past few decades, bolstering the growth of the field of microbiome research (Johnson et al., 2019). Despite its widespread use and utility, variability exists in protocols used for *16S* rRNA

sequencing with differences in the target variable region, primers, and reference database utilized being among the myriad of experimental factors that may lead to differential microbial characterization (Tang et al., 1998; Janda and Abbott, 2007; Schloss, 2010). To minimize the likelihood of inaccurate microbiome characterization, to allow for more robust comparison of *16S* data across studies, and to increase the efficient use of finite research budgets, the effects of different experimental factors on *16S* sequencing outcomes need to be better determined. To assess the impact of different sequencing depth, or effort, on octocoral microbiome analysis, 24 of the 98 total samples were sequenced at both low- and high-sequence depth on the Illumina Miseq system while attempting to keep all other factors the same.

Both the high- and low-read datasets revealed similar alpha diversity trends for all octocoral species examined. Notably, the high-read dataset did have higher alpha diversity values, but the patterns were the same with *Thesea nivea* displaying the highest alpha diversity value for both datasets and the other four octocoral species showing similar low alpha diversity values. In addition to matching patterns in alpha diversity, nMDS ordination revealed the same patterns of clustering between the high- and low-read datasets with every octocoral sample clustered by species, notably with *Scleracis* sp. (Red) and *Scleracis* sp. (Yellow) clustering together in both datasets. Although the six most abundant microbial classes between all the samples were the same for both the high- and low-read datasets, the distribution of prevalence of microbial taxa differed between the datasets. In summary the alpha diversity patterns and clustering of microbiomes was the same, but the distribution of microbial taxa in the microbiomes differed between both datasets. These differences in microbiome community composition between datasets may be explained by the differences in the sequence depth, DNA

amount used in the sequencing, degradation of sample DNA between runs, or a combination of the three.

As the high- and low-read datasets are meant to only be different in sequence depth, the difference in microbiome community composition is potentially due to only sequence depth differences as reviews have highlighted the significant influence sequence depth has on microbiome community outcomes. The different microbial taxa abundances is explainable as diversity studies in ecology have long found that the more you sample the more rare taxa you identify, in other words sampling effort can dictate the biological result of population surveys (Lande, 1996). This effect of sampling effort, in this case read count, has been shown with microbial taxa where greater sequence depth led to greater taxa discovery with next-generation sequencing reads (Zaheer et al., 2018), lending to the potential differential abundances of microbial taxa identified in this *16S* sequencing study along with the differences in alpha diversity values (e.g. *Thesea nivea* high 5.174, *Thesea nivea* low 4.616) between both datasets (Table 7).

Other factors that may have played a role include input DNA amounts, which can alter *16S* derived microbiome community structures (Pollock et al., 2018). For example, low input DNA amounts in *16S* sequence runs can lead the to the misrepresentation of certain taxa abundances and therefore community structure, by overestimating some microbial taxa abundance and underestimating others (Multinu et al., 2018). This effect of DNA input amount is noteworthy as the high and low runs in this study were performed months apart on the same extracted DNA samples, meaning that separate normalization dilutions between 1 to 5 ng μl^{-1} were performed when prepping plates, therefore slightly different input amounts of DNA were

likely used between the high and low runs. Pipetting error may also contribute to this DNA input loading effect.

Temperature fluctuations and freeze-thaw cycles during storage of the extracted DNA may have impacted the results, as freeze-thaw cycles have been shown to breakdown DNA in storage over time (Ross et al., 1990). Skin microbiome samples showed changes in microbiome taxa abundance when samples were exposed to different durations of cold storage, similar to this studies outcomes (Klymiuk et al., 2016). That said, other work has found variable storage conditions do not affect *16S* alpha diversity or microbial operational taxonomic unit profiles (Kawada et al., 2019). In this study, the consistency between high and low runs results and the USNM samples with our collected samples implies that storage quality and duration was not an issue. Other confounding factors such as sample handling during shipment or sequencing may explain these differences as well. It is recommended that future work looking into sequence depth differences should aim to sequence samples at the same time to minimize this potential source of variability in input DNA and sample storage. Additionally, only a relatively small set of samples (n = 24) were examined for this high- versus low- sequence depth analysis. Future studies could expand upon the number of samples or even increase the number of high- and low-sequence runs to further improve the robustness of these comparisons. Lastly, despite the difference in microbial taxa abundance, this study highlights the robustness of *16S* as a method as it was able to consistently identify the microbiome trends between the two datasets despite potential differences in template DNA amount or quality and known differences in sequence depth.

Broader Impact

The results of this study have shown that the microbiomes of octocorals in this region appear to be healthy microbiomes dominated by several core microbial taxa, and that these microbiomes are spatiotemporally stable as indicated by the predominant microbial taxa and PERMANOVA results. The western GoM is home to a long-standing and economically important fishery whose target species rely upon MCEs (Adams et al., 2004; Streich et al., 2017). As the region is consistently facing the effects of anthropogenic activity, such as oil spills and consistent litter pollution even at deeper depths, there is a need for novel management practices (Wei et al., 2012; White et al., 2012). The growing use of sequence and omics-based approaches holds the potential to improve management of rarely seen yet vital habitat like these MCEs. From the results of this work another metric for monitoring the health and understanding the biology of octocorals comprising mesophotic coral ecosystems has been provided.

The results of this study support that more research should be put into standardizing *16S* rRNA sequencing protocols, with further examination of the effects of all experimental parameters on sequence results to allow for stronger cross comparisons of microbiome studies. Despite this need for more research, this study indicates that to balance cost with research outcomes it is appropriate to opt for low-read depth sequencing when looking to only observe trends in microbiome characteristics, but when microbial taxa profiling is desired a higher read depth sequence approach should be taken.

CHAPTER V

CONCLUSION

The study and assessment of octocorals at mesophotic depths in the GoM is still in its nascency. This study provides the first characterization of bacterial and archaeal taxa present in the microbiomes of thirteen octocoral groups sampled primarily along the STB and FGB (Objective 1). Octocoral microbiomes from these regions showed similarity across all octocoral groups with a few core predominant microbial taxa making up the majority of the microbiomes. Alphaproteobacteria, Gammaproteobacteria, Mollicutes, Nitrosospheria, and Spirochaetia were the predominant microbial class seen. At the generic level, *Endozoicomonas, Mycoplasma, Nitrosopumilus, Spirochaeta* were generally the most predominant microbial groups observed. As these microbial groups are considered to be indicators of good health in octocoral microbiomes, potentially serving roles like nitrification and protein cycling for their hosts, the results from this study suggest healthy octocorals inhabit these MCEs. That said, the pathogenic microbial genus *Vibrio* was one of the more abundant microbes in the microbiome of *Bebryce* potentially indicating this group was less healthy than others and thus may be a priority for future studies. The microbiomes of octocorals also showed low alpha diversity for eleven of the thirteen octocoral groups, with *Bebryce* and *Thesea nivea* being the two exceptions. This generally low alpha diversity is in agreement with previous literature on octocoral microbiomes from the

Mediterranean and Caribbean showing low alpha diversity, core predominant microbes, and consistently predominant microbial taxa.

Clustering of the octocoral microbiomes using nMDS on Bray Curtis distances revealed that microbiomes clustered primarily due to octocoral groups as opposed to other factors (depth, season, reef type, and region) (Objective 2) that may be important contributors to clustering within groups. Statistical analysis confirmed this significance of all factors with a multivariate PERMANOVA, that also showed that octocoral groups were the primary drivers of microbiome composition. The result indicates that phylosymbiosis is at play for western GoM mesophotic ocotocorals in agreement with literature often reporting this pattern of phylosymbiosis in octocorals globally.

As a rule the deeper your sequence depth the greater rare taxa are highlighted, and the more accurate the taxa representation becomes in the microbiome. The subset of preliminary octocoral samples run at low- and high-sequence depth revealed nMDS clustering and alpha diversity metrics were the same between the high- and low-read groups. However, predominant and identified microbial taxa differed significantly between the two datasets. Different microbial taxa identified between low- and high-read samples are thought to be due to differences in sampling effort, or sequence depth, between the two groups but other factors may be at play. These data can help guide researchers studying octocoral microbiomes in determining the appropriate depth at which to sequence for the purpose of their studies. Specifically, that higher read depths are more appropriate for studying rare microbial taxa within microbiomes and that low read depths are sufficient for characterizing overall trends.

Overall, this study has brough forth a greater understanding of octocorals comprising wester GoM MCEs and provided a potential metric for monitoring their long-term health. While the microbiomes presently indicate octocorals in this region are healthy, further efforts should be made to increase the scope of microbiome assessment in this region for these foundational organisms to increase the robustness of microbiomes as a monitoring and conservation tool.

REFERENCES

Adams, C. M., E. Hernandez and J. C. Cato (2004). "The economic significance of the Gulf of Mexico related to population, income, employment, minerals, fisheries and shipping." Ocean & Coastal Management **47**(11-12): 565-580.

Anderson, M. J. (2014). "Permutational multivariate analysis of variance (PERMANOVA)." Wiley statsref: Statistics Reference Online 1-15.

Apprill, A., McNally, S., Parsons, R., & Weber, L. (2015). “Minor revision to V4 region SSU rRNA 806R gene primer greatly increases detection of SAR11 bacterioplankton.” Aquatic Microbial Ecology **75(2)**: 129-137.

Arotsker, L., N. Siboni, E. Ben-Dov, E. Kramarsky-Winter, Y. Loya and A. Kushmaro (2009). "Vibrio sp. as a potentially important member of the Black Band Disease (BBD) consortium in Favia sp. corals." FEMS Microbiology Ecology **70**(3): 515-524.

Bahrndorff, S., T. Alemu, T. Alemneh and J. Lund Nielsen (2016). "The Microbiome of Animals: Implications for Conservation Biology." International Journal of Genomics **2016**: 5304028.

Baillon, S., J.-F. Hamel, V. E. Wareham and A. Mercier (2012). "Deep cold-water corals as nurseries for fish larvae." Frontiers in Ecology and the Environment **10**(7): 351-356.

Baldwin, C. C., L. Tornabene and D. R. Robertson (2018). "Below the Mesophotic." Scientific Reports **8**(1): 4920.

Bayer, B., Vojvoda, J., Offre, P. et al. (2016). Physiological and genomic characterization of two novel marine thaumarchaeal strains indicates niche differentiation. ISME J **10**, 1051–1063.

Bayer, T., C. Arif, C. Ferrier-Pagès, D. Zoccola, M. Aranda and C. R. Voolstra (2013). "Bacteria of the genus Endozoicomonas dominate the microbiome of the Mediterranean gorgonian coral Eunicella cavolini." Marine Ecology Progress Series **479**: 75-84.

Belopolsky, A. V. and A. W. Droxler (1999). Uppermost Pleistocene Transgressive Coralgal Reefs on the Edge of the South Texas Shelf: Analogs for Reefal Reservoirs Buried in Siliciclastic Shelves. Advanced Reservoir Characterization for the 21st Century. T. F. Hentz, SEPM Society for Sedimentary Geology. **19:** 0.

Blakeway, R. D., A. Q. Fogg, M. A. Johnston, J. R. Rooker and G. A. Jones (2022). "Key Life History Attributes and Removal Efforts of Invasive Lionfish (Pterois volitans) in the Flower Garden Banks National Marine Sanctuary, Northwestern Gulf of Mexico." Frontiers in Marine Science **9**.

Blyth-Skyrme, V., J. J. B. Rooney, F. A. Parrish and R. C. Boland (2013). "Mesophotic coral ecosystems: potential candidates as essential fish habitat and habitat areas of particular concern."

Bongiorni, L., M. Mea, C. Gambi, A. Pusceddu, M. Taviani and R. Danovaro (2010). "Deep-water scleractinian corals promote higher biodiversity in deep-sea meiofaunal assemblages along continental margins." Biological Conservation **143**(7): 1687-1700.

Bourne, D. G., K. M. Morrow and N. S. Webster (2016). "Insights into the coral microbiome: underpinning the health and resilience of reef ecosystems." Annual Review Microbioly **70**(1): 317-340.

Bridge, T. C. L., T. P. Hughes, J. M. Guinotte and P. Bongaerts (2013). "Call to protect all coral reefs." Nature Climate Change **3**(6): 528-530.

Bright, T. J. and R. Rezak (1977). Chapter 6 Reconnaissance of Reefs and Fishing Banks of the Texas Continental Shelf. Elsevier Oceanography Series. R. A. Geyer, Elsevier. **17:** 113-150.

Bright, T., D. McGrail, R. Rezak, G. Boland and A. Trippett (1985). "The Flower Gardens: A compendium of information." OCS Study MMS 85-0024.

Cairns, S. D. (2007). "Deep-water corals: an overview with special reference to diversity and distribution of deep-water scleractinian corals." Bulletin of Marine Science **81**(3): 311-322.

Callahan, B. J., P. J. McMurdie, M. J. Rosen, A. W. Han, A. J. A. Johnson and S. P. Holmes (2016). "DADA2: High-resolution sample inference from Illumina amplicon data." Nature Methods **13**(7): 581-583.

Caporaso, J. G., J. Kuczynski, J. Stombaugh, K. Bittinger, F. D. Bushman, E. K. Costello, N. Fierer, A. G. Peña, J. K. Goodrich, J. I. Gordon, G. A. Huttley, S. T. Kelley, D. Knights, J. E. Koenig, R. E. Ley, C. A. Lozupone, D. McDonald, B. D. Muegge, M. Pirrung, J. Reeder, J. R. Sevinsky, P. J. Turnbaugh, W. A. Walters, J. Widmann, T. Yatsunenko, J. Zaneveld and R. Knight (2010). "QIIME allows analysis of high-throughput community sequencing data." Nature Methods **7**(5): 335-336.

Chao, A. (1984). "Nonparametric estimation of the number of classes in a population." Scandinavian Journal of Statistics 265-270.

Chen, Z., P. C. Hui, M. Hui, Y. K. Yeoh, P. Y. Wong, M. C. W. Chan, M. C. S. Wong, S. C. Ng, F. K. L. Chan and P. K. S. Chan (2019). "Impact of Preservation Method and 16S rRNA Hypervariable Region on Gut Microbiota Profiling." mSystems **4**(1): e00271-00218.

Corinaldesi, C., S. Varrella, M. Tangherlini, A. Dell'Anno, S. Canensi, C. Cerrano and R. Danovaro (2022). "Changes in coral forest microbiomes predict the impact of marine

heatwaves on habitat-forming species down to mesophotic depths." Science of The Total Environment **823**: 153701.

Correa, H., B. Haltli, C. Duque and R. Kerr (2013). "Bacterial Communities of the Gorgonian Octocoral Pseudopterogorgia elisabethae." Microbial Ecology **66**(4): 972-985.

Deignan, L. K., K. H. Pwa, A. A. R. Loh, S. A. Rice and D. McDougald (2023). "The microbiomes of two Singaporean corals show site-specific differentiation and variability that correlates with the seasonal monsoons." Coral Reefs **42**: 677–691.

Dunphy, C. M., T. C. Gouhier, N. D. Chu and S. V. Vollmer (2019). "Structure and stability of the coral microbiome in space and time." Scientific Reports **9**(1): 6785.

Durazzi, F., C. Sala, G. Castellani, G. Manfreda, D. Remondini and A. De Cesare (2021). "Comparison between 16S rRNA and shotgun sequencing data for the taxonomic characterization of the gut microbiota." Scientific Reports **11**(1): 3030.

Etnoyer, P. J., L. N. Wickes, M. Silva, J. D. Dubick, L. Balthis, E. Salgado and I. R. MacDonald (2016). "Decline in condition of gorgonian octocorals on mesophotic reefs in the northern Gulf of Mexico: before and after the Deepwater Horizon oil spill." Coral Reefs **35**(1): 77-90.

Fraher, M. H., P. W. O'toole and E. M. Quigley (2012). "Techniques used to characterize the gut microbiota: a guide for the clinician." Nature Reviews Gastroenterology & Hepatology **9**(6): 312-322.

Fuchs, L., H. Schmeling and H. Koyi (2011). "Numerical models of salt diapir formation by down-building: the role of sedimentation rate, viscosity contrast, initial amplitude and wavelength." Geophysical Journal International **186**(2): 390-400.

Gil-Agudelo, D. L., C. E. Cintra-Buenrostro, J. Brenner, P. González-Díaz, W. Kiene, C. Lustic and H. Pérez-España (2020). "Coral Reefs in the Gulf of Mexico Large Marine Ecosystem: Conservation Status, Challenges, and Opportunities." Frontiers in Marine Science **6**.

Glasl, B., P. Bongaerts, N. H. Elisabeth, O. Hoegh-Guldberg, G. J. Herndl and P. R. Frade (2017). "Microbiome variation in corals with distinct depth distribution ranges across a shallow–mesophotic gradient (15–85 m)." Coral Reefs **36**(2): 447-452.

Gray, M. A., R. P. Stone, M. R. McLaughlin and C. A. Kellogg (2011). "Microbial consortia of gorgonian corals from the Aleutian islands." FEMS Microbiology Ecology **76**(1): 109-120.

Gweon, H. S., L. P. Shaw, J. Swann, N. De Maio, M. AbuOun, R. Niehus, A. T. M. Hubbard, M. J. Bowes, M. J. Bailey, T. E. A. Peto, S. J. Hoosdally, A. S. Walker, R. P. Sebra, D. W. Crook, M. F. Anjum, D. S. Read, N. Stoesser, M. Abuoun, M. Anjum, M. J. Bailey, L.

Barker, H. Brett, M. J. Bowes, K. Chau, D. W. Crook, N. De Maio, D. Gilson, H. S. Gweon, A. T. M. Hubbard, S. Hoosdally, J. Kavanagh, H. Jones, T. E. A. Peto, D. S. Read, R. Sebra, L. P. Shaw, A. E. Sheppard, R. Smith, E. Stubberfield, J. Swann, A. S. Walker, N. Woodford and R. c. on behalf of the (2019). "The impact of sequencing depth on the inferred taxonomic composition and AMR gene content of metagenomic samples." Environmental Microbiome **14**(1): 7.

Hadaidi, G., T. Röthig, L. K. Yum, M. Ziegler, C. Arif, C. Roder, J. Burt and C. R. Voolstra (2017). "Stable mucus-associated bacterial communities in bleached and healthy corals of Porites lobata from the Arabian Seas." Scientific Reports **7**(1): 45362.

Hamilton, P., G. S. Fargion and D. C. Biggs (1999). "Loop Current Eddy Paths in the Western Gulf of Mexico." Journal of Physical Oceanography **29**(6): 1180-1207.

Harder, T., S. C. K. Lau, S. Dobretsov, T. K. Fang and P.-Y. Qian (2003). "A distinctive epibiotic bacterial community on the soft coral Dendronephthya sp. and antibacterial activity of coral tissue extracts suggest a chemical mechanism against bacterial epibiosis." FEMS Microbiology Ecology **43**(3): 337-347.

Haydon, T. D., D. J. Suggett, N. Siboni, T. Kahlke, E. F. Camp and J. R. Seymour (2022). "Temporal Variation in the Microbiome of Tropical and Temperate Octocorals." Microbial Ecology **83**(4): 1073-1087.

Hickerson, E. L., G. P. Schmahl, M. L. Robbart, W. F. Precht and C. Caldow (2005). "State of Coral Reef Ecosystems of the Flower Garden Banks , Stetson Bank , and Other Banks in the Northwestern Gulf of Mexico."

Hickerson, E. L., G. Schmahl, M. Robbart, W. F. Precht and C. Caldow (2008). "The state of coral reef ecosystems of the Flower Garden Banks, Stetson Bank, and other banks in the northwestern Gulf of Mexico." The state of coral reef ecosystems of the United States and Pacific Freely Associated States 189-217.

Hollander, M., D. A. Wolfe and E. Chicken (2013). "Nonparametric statistical methods." John Wiley & Sons.

Hudec, M. R. and M. P. A. Jackson (2007). "Terra infirma: Understanding salt tectonics." Earth-Science Reviews **82**(1): 1-28.

Hunt, L. R., S. M. Smith, K. R. Downum and L. D. Mydlarz (2012). "Microbial regulation in gorgonian corals." Marine Drugs **10**(6): 1225-1243.

Janda, J. M. and S. L. Abbott (2007). "16S rRNA gene sequencing for bacterial identification in the diagnostic laboratory: pluses, perils, and pitfalls." Journal of Clinical Microbioly **45**(9): 2761-2764.

Jiang, Y., Y. Jiang, S. Wang, Q. Zhang and X. Ding (2019). "Optimal sequencing depth design for whole genome re-sequencing in pigs." BMC Bioinformatics **20**(1): 556.

Johnson, J. S., D. J. Spakowicz, B.-Y. Hong, L. M. Petersen, P. Demkowicz, L. Chen, S. R. Leopold, B. M. Hanson, H. O. Agresta, M. Gerstein, E. Sodergren and G. M. Weinstock (2019). "Evaluation of 16S rRNA gene sequencing for species and strain-level microbiome analysis." Nature Communications **10**(1): 5029.

Johnston, M. A., J. A. Embesi, R. J. Eckert, M. F. Nuttall, E. L. Hickerson and G. P. Schmahl (2016). "Persistence of coral assemblages at East and West Flower Garden Banks, Gulf of Mexico." Coral Reefs **35**(3): 821-826.

Johnston, M. A., K. O'Connell, R. D. Blakeway, J. MacMillan, M. F. Nuttall, X. Hu, J. A. Embesi, E. L. Hickerson and G. P. Schmahl (2021). "Long-Term Monitoring at East and West Flower Garden Banks: 2019 Annual Report."

Johnston, M. A., M. S. Studivan, I. C. Enochs, A. M. S. Correa, N. Besemer, R. J. Eckert, K. Edwards, R. Hannum, X. Hu, M. Nuttall, K. O'Connell, A. M. Palacio-Castro, G. P. Schmahl, A. B. Sturm, B. Ushijima and J. D. Voss (2023). "Coral disease outbreak at the remote Flower Garden Banks, Gulf of Mexico." Frontiers in Marine Science **10**.

Jovel, J., J. Patterson, W. Wang, N. Hotte, S. O'Keefe, T. Mitchel, T. Perry, D. Kao, A. L. Mason, K. L. Madsen and G. K.-S. Wong (2016). "Characterization of the Gut Microbiome Using 16S or Shotgun Metagenomics." Frontiers in Microbiology **7**.

Kawada, Y., Y. Naito, A. Andoh, M. Ozeki and R. Inoue (2019). "Effect of storage and DNA extraction method on 16S rRNA-profiled fecal microbiota in Japanese adults." Journal of Clinical Biochemistry and Nutrition **64**(2): 106-111.

Keller-Costa, T., A. Lago-Lestón, J. P. Saraiva, R. Toscan, S. G. Silva, J. Gonçalves, C. J. Cox, N. Kyrpides, U. Nunes da Rocha and R. Costa (2021). "Metagenomic insights into the taxonomy, function, and dysbiosis of prokaryotic communities in octocorals." Microbiome **9**(1): 72.

Kellogg, C. A., J. T. Lisle and J. P. Galkiewicz (2009). "Culture-independent characterization of bacterial communities associated with the cold-water coral *Lophelia pertusa* in the northeastern Gulf of Mexico." Applied and Environmental Microbiology **75**(8): 2294-2303.

Klymiuk, I., I. Bambach, V. Patra, S. Trajanoski and P. Wolf (2016). "16S based microbiome analysis from healthy subjects' skin swabs stored for different storage periods reveal phylum to genus level changes." Frontiers in microbiology **7**: 2012.

Kozich, J. J., Westcott, S. L., Baxter, N. T., Highlander, S. K., & Schloss, P. D. (2013). "Development of a dual-index sequencing strategy and curation pipeline for analyzing

amplicon sequence data on the MiSeq Illumina sequencing platform." Applied and Environmental Microbiology **79(17)**: 5112-5120.

Kruskal, J. B. (1964). "Nonmetric multidimensional scaling: a numerical method." Psychometrika **29**(2): 115-129.

La Rivière, M., J. Garrabou and M. Bally (2013). "Interspecific comparisons of host-associated bacterial diversity support coevolution of Hahellaceae and gorgonian corals." Rapp Comm Int Mer Médit **40**: 388.

Lahti, L., S. Shetty, T. Blake and J. Salojarvi (2017). "Tools for microbiome analysis in R Version 2.1. 26."

LaJeunesse, T. C. (2020). "Zooxanthellae." Current Biology **30**(19): R1110-R1113.

Lande, R. (1996). "Statistics and partitioning of species diversity, and similarity among multiple communities." Oikos 5-13.

Laverick, J. H., D. A. Andradi-Brown and A. D. Rogers (2017). "Using light-dependent scleractinia to define the upper boundary of mesophotic coral ecosystems on the reefs of Utila, Honduras." PLoS One **12**(8): e0183075.

Lilburn, T. G., K. S. Kim, N. E. Ostrom, K. R. Byzek, J. R. Leadbetter and J. A. Breznak (2001). "Nitrogen Fixation by Symbiotic and Free-Living Spirochetes." Science **292**(5526): 2495-2498.

Lim, S. J. and S. R. Bordenstein (2020). "An introduction to phylosymbiosis." Proceedings of the Royal Society B **287**(1922): 20192900.

Limer, B. D., J. Bloomberg and D. M. Holstein (2020). "The Influence of Eddies on Coral Larval Retention in the Flower Garden Banks." Frontiers in Marine Science **7**.

Lundin, D., I. Severin, J. B. Logue, Ö. Östman, A. F. Andersson and E. S. Lindström (2012). "Which sequencing depth is sufficient to describe patterns in bacterial α- and β-diversity?" Environmental Microbiology Reports **4**(3): 367-372.

Marchesi, J. R. and J. Ravel (2015). "The vocabulary of microbiome research: a proposal." Microbiome **3**(1): 31.

McCauley, E. P., B. Haltli, H. Correa and R. G. Kerr (2016). "Spatial and temporal investigation of the microbiome of the Caribbean octocoral Erythropodium caribaeorum." Fems Microbiology Ecology **92**(9).

McCauley, M., C. R. Jackson and T. L. Goulet (2020). "Microbiomes of Caribbean Octocorals Vary Over Time but Are Resistant to Environmental Change." Frontiers in Microbiology **11**.

McDevitt-Irwin, J. M., J. K. Baum, M. Garren and R. L. Vega Thurber (2017). "Responses of coral-associated bacterial communities to local and global stressors." Frontiers in Marine Science 262.

McFadden, C. S., L. P. van Ofwegen and A. M. Quattrini (2022). "Revisionary systematics of Octocorallia (Cnidaria: Anthozoa) guided by phylogenomics." Bulletin of the Society of Systematic Biologists **1**(3).

McMurdie, P. J. and S. Holmes (2015). "Shiny-phyloseq: Web application for interactive microbiome analysis with provenance tracking." Bioinformatics **31**(2): 282-283.

Mills, E., K. Shechtman, Y. Loya and E. Rosenberg (2013). "Bacteria appear to play important roles in both causing and preventing the bleaching of the coral Oculina patagonica." Marine Ecology Progress Series **489**: 155-162.

Multinu, F., S. C. Harrington, J. Chen, P. R. Jeraldo, S. Johnson, N. Chia and M. R. Walther-Antonio (2018). "Systematic Bias Introduced by Genomic DNA Template Dilution in 16S rRNA Gene-Targeted Microbiota Profiling in Human Stool Homogenates." mSphere **3**(2).

Nash, H., S. Magnuson and J. J. Tunnell (2013). "What is Known About Species Richness and Distribution on the Outer-Shelf South Texas Banks?" Gulf and Caribbean Research **25**: 9-18.

Neave, M. J., A. Apprill, C. Ferrier-Pagès and C. R. Voolstra (2016). "Diversity and function of prevalent symbiotic marine bacteria in the genus Endozoicomonas." Applied Microbiology and Biotechnology **100**(19): 8315-8324.

Neely, K. L., K. A. Macaulay, E. K. Hower and M. A. Dobler (2020). "Effectiveness of topical antibiotics in treating corals affected by Stony Coral Tissue Loss Disease." PeerJ 2020 Jun 9;8:e9289.

Oksanen, J., R. Kindt, P. Legendre, B. O'Hara, M. H. H. Stevens, M. J. Oksanen and M. Suggests (2007). "The vegan package." Community ecology package **10**(631-637): 719.

Pacific Islands Fisheries Science Center Administrative Report H 13-02

Parada, Alma E., David M. Needham, and Jed A. Fuhrman (2016). "Every base matters: assessing small subunit rRNA primers for marine microbiomes with mock communities, time series and global field samples." Environmental Microbiology **18.5**: 1403-1414.

Pavliska, C. L. (2019). "DNA Barcoding Reveals Unexpected Diversity in Octocorallia in the Northwestern Gulf of Mexico." M.S., The University of Texas Rio Grande Valley.

Peixoto, R. S., M. Sweet, H. D. Villela, P. Cardoso, T. Thomas, C. R. Voolstra, L. Høj and D. G. Bourne (2021). "Coral probiotics: premise, promise, prospects." Annual Review of Animal Biosciences **9**: 265-288.

Pollock, F. J., R. McMinds, S. Smith, D. G. Bourne, B. L. Willis, M. Medina, R. V. Thurber and J. R. Zaneveld (2018). "Coral-associated bacteria demonstrate phylosymbiosis and cophylogeny." Nature Communications **9**(1): 4921.

Pollock, J., L. Glendinning, T. Wisedchanwet and M. Watson (2018). "The madness of microbiome: attempting to find consensus "best practice" for 16s microbiome studies." Applied and Environmental Microbiology **84**(7): e02627-02617.

Quast, C., E. Pruesse, P. Yilmaz, J. Gerken, T. Schweer, P. Yarza, J. Peplies and F. O. Glöckner (2013). "The SILVA ribosomal RNA gene database project: improved data processing and web-based tools." Nucleic Acids Research **41**(Database issue): D590-D596.

Rädecker, N., C. Pogoreutz, C. R. Voolstra, J. Wiedenmann and C. Wild (2015). "Nitrogen cycling in corals: the key to understanding holobiont functioning?" Trends in Microbiology **23**(8): 490-497.

Ramakodi, M. P. (2022). "Influence of 16S rRNA reference databases in amplicon-based environmental microbiome research." Biotechnology Letters **44**(3): 523-533.

Ransome, E., S. J. Rowley, S. Thomas, K. Tait and C. B. Munn (2014). "Disturbance to conserved bacterial communities in the cold-water gorgonian coral Eunicella verrucosa." FEMS Microbiology Ecology **90**(2): 404-416.

Register, F. (2021). "Expansion of Flower Garden Banks National Marine Sanctuary." Washington, DC: NOAA.

Rezak, R., S. R. Gittings and T. J. Bright (2015). "Biotic Assemblages and Ecological Controls on Reefs and Banks of the Northwest Gulf of Mexico." American Zoologist **30**(1): 23-35.

Richard, S. N. (2005). "Population characteristics of a recovering US Virgin Islands red hind spawning aggregation following protection." Marine Ecology Progress Series **286**: 81-97.

Ritchie, K. B., B. D. Keller and E. D. Estevez (2008). A scientific forum on the Gulf of Mexico: the islands in the stream concept, Mote Marine Laboratory, Sarasota, FL.

Roberts, J. M., A. J. Wheeler and A. Freiwald (2006). "Reefs of the Deep: The Biology and Geology of Cold-Water Coral Ecosystems." Science **312**(5773): 543-547.

Robertson, V., B. Haltli, E. P. McCauley, D. P. Overy and R. G. Kerr (2016). "Highly Variable Bacterial Communities Associated with the Octocoral Antillogorgia elisabethae." Microorganisms **4**(3).

Rocha, L. A., H. T. Pinheiro, B. Shepherd, Y. P. Papastamatiou, O. J. Luiz, R. L. Pyle and P. Bongaerts (2018). "Mesophotic coral ecosystems are threatened and ecologically distinct from shallow water reefs." Science **361**(6399): 281-284.

Rodriguez, R., E. E. Easton, T. C. Shirley, J. W. Tunnell and D. Hicks (2018). "Preliminary Multivariate Comparison of Coral Assemblages on Carbonate Banks in the Western Gulf of Mexico." Gulf and Caribbean Research **29**: 23-33.

Rosado, P. M., D. C. A. Leite, G. A. S. Duarte, R. M. Chaloub, G. Jospin, U. Nunes da Rocha, J. P. Saraiva, F. Dini-Andreote, J. A. Eisen, D. G. Bourne and R. S. Peixoto (2019). "Marine probiotics: increasing coral resistance to bleaching through microbiome manipulation." The ISME Journal **13**(4): 921-936.

Ross, K. S., N. E. Haites and K. F. Kelly (1990). "Repeated freezing and thawing of peripheral blood and DNA in suspension: effects on DNA yield and integrity." J Med Genet **27**(9): 569-570.

Sahl, L. E., W. J. Merrell, D. W. McGrail and J. A. Webb (1987). "Transport of mud on continental shelves: Evidence from the Texas Shelf." Marine Geology **76**: 33-43.

Sammarco, P. W., M. J. Risk, H. Schwarcz and J. Heikoop (1999). "Cross-continental shelf trends in coral δ15N on the Great Barrier Reef: further consideration of the reef nutrient paradox." Marine Ecology Progress Series **180**: 131-138.

Schloss, P. D. (2010). "The Effects of Alignment Quality, Distance Calculation Method, Sequence Filtering, and Region on the Analysis of 16S rRNA Gene-Based Studies." PLOS Computational Biology **6**(7): e1000844.

Shannon, C. E. (1948). "A mathematical theory of communication." The Bell System Technical Journal **27**(3): 379-423.

Shideler, G. L. (1981). "Development of the benethic nepheloid layer on the south Texas continental shelf, western Gulf of Mexico." Marine Geology **41**(1): 37-61.

Siboni, N., E. Ben-Dov, A. Sivan and A. Kushmaro (2008). "Global distribution and diversity of coral-associated Archaea and their possible role in the coral holobiont nitrogen cycle." Environmental Microbiology **10**(11): 2979-2990.

Silverman, J. D., R. J. Bloom, S. Jiang, H. K. Durand, E. Dallow, S. Mukherjee and L. A. David (2021). "Measuring and mitigating PCR bias in microbiota datasets." PLOS Computational Biology **17**(7): e1009113.

Slattery, M., M. P. Lesser, D. Brazeau, M. D. Stokes and J. J. Leichter (2011). "Connectivity and stability of mesophotic coral reefs." Journal of Experimental Marine Biology and Ecology **408**(1): 32-41.

Smith, T. B., J. Gyory, M. E. Brandt, W. J. Miller, J. Jossart and R. S. Nemeth (2016). "Caribbean mesophotic coral ecosystems are unlikely climate change refugia." Global Change Biology **22**(8): 2756-2765.

Streich, M. K., M. J. Ajemian, J. J. Wetz and G. W. Stunz (2017). "A comparison of fish community structure at mesophotic artificial reefs and natural banks in the western Gulf of Mexico." Marine and Coastal Fisheries **9**(1): 170-189.

Sussman, M., B. L. Willis, S. Victor and D. G. Bourne (2008). "Coral pathogens identified for white syndrome (WS) epizootics in the Indo-Pacific." PLoS One **3**(6): e2393.

Tang, Y.-W., N. M. Ellis, M. K. Hopkins, D. H. Smith, D. E. Dodge and D. H. Persing (1998). "Comparison of Phenotypic and Genotypic Techniques for Identification of Unusual Aerobic Pathogenic Gram-Negative Bacilli." Journal of Clinical Microbiology **36**(12): 3674-3679.

van de Water, J. A. J. M., R. Melkonian, C. R. Voolstra, H. Junca, E. Beraud, D. Allemand and C. Ferrier-Pagès (2017). "Comparative Assessment of Mediterranean Gorgonian-Associated Microbial Communities Reveals Conserved Core and Locally Variant Bacteria." Microbial Ecology **73**(2): 466-478.

van de Water, J., C. R. Voolstra, C. Rottier, S. Cocito, A. Peirano, D. Allemand and C. Ferrier-Pagès (2018). "Seasonal Stability in the Microbiomes of Temperate Gorgonians and the Red Coral Corallium rubrum Across the Mediterranean Sea." Microbial Ecology **75**(1): 274-288.

van de Water, J., D. Allemand and C. Ferrier-Pages (2018). "Host-microbe interactions in octocoral holobionts - recent advances and perspectives." Microbiome **6**.

van Oppen, M. J. H. and L. L. Blackall (2019). "Coral microbiome dynamics, functions and design in a changing world." Nature Reviews Microbiology **17**(9): 557-567.

Walters, W., Hyde, E. R., Berg-Lyons, D., Ackermann, G., Humphrey, G., Parada, A., ... & Knight, R. (2016). “Improved bacterial 16S rRNA gene (V4 and V4-5) and fungal internal transcribed spacer marker gene primers for microbial community surveys.” Msystems **1(1)**: e00009-15.

Wei, C.-L., G. T. Rowe, C. C. Nunnally and M. K. Wicksten (2012). "Anthropogenic “litter” and macrophyte detritus in the deep northern Gulf of Mexico." Marine Pollution Bulletin **64**(5): 966-973.

Welsh, R. M., J. R. Zaneveld, S. M. Rosales, J. P. Payet, D. E. Burkepile and R. V. Thurber (2016). "Bacterial predation in a marine host-associated microbiome." The ISME Journal **10**(6): 1540-1544.

West, A. G., D. W. Waite, P. Deines, D. G. Bourne, A. Digby, V. J. McKenzie and M. W. Taylor (2019). "The microbiome in threatened species conservation." Biological Conservation **229**: 85-98.

White, H. K., P.-Y. Hsing, W. Cho, T. M. Shank, E. E. Cordes, A. M. Quattrini, R. K. Nelson, R. Camilli, A. W. J. Demopoulos, C. R. German, J. M. Brooks, H. H. Roberts, W. Shedd, C. M. Reddy and C. R. Fisher (2012). "Impact of the Deepwater Horizon oil spill on a deep-water coral community in the Gulf of Mexico." Proceedings of the National Academy of Sciences **109**(50): 20303-20308.

Wilhelm, R. C., H. M. van Es and D. H. Buckley (2022). "Predicting measures of soil health using the microbiome and supervised machine learning." Soil Biology and Biochemistry **164**: 108472.

Wilmanski, T., C. Diener, N. Rappaport, S. Patwardhan, J. Wiedrick, J. Lapidus, J. C. Earls, A. Zimmer, G. Glusman, M. Robinson, J. T. Yurkovich, D. M. Kado, J. A. Cauley, J. Zmuda, N. E. Lane, A. T. Magis, J. C. Lovejoy, L. Hood, S. M. Gibbons, E. S. Orwoll and N. D. Price (2021). "Gut microbiome pattern reflects healthy ageing and predicts survival in humans." Nature Metabolism **3**(2): 274-286.

Zaheer, R., N. Noyes, R. Ortega Polo, S. R. Cook, E. Marinier, G. Van Domselaar, K. E. Belk, P. S. Morley and T. A. McAllister (2018). "Impact of sequencing depth on the characterization of the microbiome and resistome." Scientific Reports **8**(1): 5890.

Zheng, C.-J., C.-L. Shao, M. Chen, Z.-G. Niu, D.-L. Zhao and C.-Y. Wang (2015). "Merosesquiterpenoids and Ten-Membered Macrolides from a Soft Coral-Derived Lophiostoma sp. Fungus." Chemistry & Biodiversity **12**(9): 1407-1414.

Zinicola, M., H. Higgins, S. Lima, V. Machado, C. Guard and R. Bicalho (2015). "Shotgun Metagenomic Sequencing Reveals Functional Genes and Microbiome Associated with Bovine Digital Dermatitis." Plos One **10**(7): e0133674.

APPENDIX A

APPENDIX A

TABLES

Table 1. Octocoral Sample Summary

Collection information for 98 octocoral samples used in this study. Whether high and low sequence data exists for each sample is indicated (N is only low sequence depth, Y is high and low sequence depth).

Sample ID	Octocoral Species	Collection Site	Date (DD/MM/YY)	Latitude	Longitude	Collection Method	High and Low Read
DFH32-515L	*Scleracis* Yellow	McGrail Bank	23/09/17	27.9510035	-92.5428005	ROV	Y
DFH32-526B	*Scleracis* Yellow	Elvers Bank	25/09/17	27.8400120	-92.9203153	ROV	Y
DFH35-634A	*Scleracis* Yellow	Geyer Bank	25/07/18	27.7861950	-93.0717080	ROV	Y
DFH35-635B	*Scleracis* Yellow	Bright Bank	25/07/18	27.9106080	-93.6589740	ROV	Y
DFH35-640B	*Scleracis* Yellow	Bright Bank	26/07/18	27.9062220	-93.3423730	ROV	Y
DFH32-511D	*Scleracis* Red	Alderdice Bank	23/09/17	28.0903013	-91.9863115	ROV	Y
DFH33-537A	*Scleracis* Red	MacNeil Bank	29/09/17	28.0159030	-93.5196650	ROV	Y
DFH35-640C1	*Scleracis* Red	Bright Bank	26/07/18	27.9062050	-93.3423980	ROV	Y
DFH37-657D	*Scleracis* Red	Parker Bank	08/09/18	27.9631497	-91.9991551	ROV	Y
DRB1_A01	*Scleracis* Red	Dream Bank	23/09/12	27.0457388	-96.7024391	ROV	Y
DRB1_A03	*Scleracis* Red	Dream Bank	23/09/12	27.0406967	-96.7060194	ROV	N
NHB1_A05	cf. *Paracis* enopla clade 1	N Hospital Bank	11/07/17	27.5774000	-96.4769000	ROV	Y
NHB1_A07	cf. *Paracis* enopla clade 1	N Hospital Bank	11/07/17	27.5774000	-96.4769000	ROV	Y
NHB1_A09	cf. *Paracis* enopla clade 1	N Hospital Bank	11/07/17	27.5774000	-96.4769000	ROV	Y
NHB2_A02	cf. *Paracis* enopla clade 1	N Hospital Bank	11/07/17	27.5774000	-96.4769000	ROV	Y

Table 1, Cont.

DRB1_A04	cf. *Paracis* enopla clade 1	Dream Bank	23/09/12	27.0375487	-96.7044178	ROV	Y
NHB1_A4	cf. *Paracis* enopla clade 1	N Hospital Bank	11/07/17	27.5774000	-96.4769000	ROV	N
DFH36-643B	*Thesea nivea*	Stetson Bank	29/07/18	28.1618981	-94.3090725	ROV	N
DFH33-536A	*Thesea nivea*	MacNeil Bank	29/09/17	28.0410090	-93.4993300	ROV	Y
DFH36-643A	*Thesea nivea*	Stetson Bank	29/07/18	28.0026310	-94.3005810	ROV	Y
CLP2_A01	*Thesea nivea*	Clipper	22/08/17	26.1902680	-96.8611770	Scuba	Y
CLP2_A02	*Thesea nivea*	Clipper	22/08/17	26.1902680	-96.8611770	Scuba	Y
HII3-A08	*Thesea nivea*	High Island	17/08/15	28.2500000	-93.4800000	Scuba	Y
DFH37-653C	*Thesea nivea*	Alderdice Bank	09/07/18	28.0826150	-92.0149471	ROV	N
CLP1_B01	*Thesea nivea*	Clipper	07/08/17	26.1902680	-96.8611770	Scuba	N
CLP1_C02	*Thesea nivea*	Clipper	07/08/17	26.1902680	-96.8611770	Scuba	N
DFH32-511C	*Thesea rubra*	Alderdice Bank	23/09/17	28.0903013	-91.9863115	ROV	N
DFH35-640D	*Thesea rubra*	Stetson Bank	26/07/18	27.9066900	-93.3429290	ROV	N
DFH33-546C	*Thesea pink*	Bright Bank	30/09/17	27.9414360	-91.9722490	ROV	N
DFH37-660C	*Thesea white*	Parker Bank	09/08/18	27.9323748	-91.9527730	ROV	N
RGV_GO1	*Leptogorgia*	RGV Reef	17/08/21	26.1645960	-97.0247440	Scuba	N
RGV_GO2	*Leptogorgia*	RGV Reef	17/08/21	26.1645960	-97.0247440	Scuba	N
RGV_GO3	*Leptogorgia*	RGV Reef	17/08/21	26.1645960	-97.0247440	Scuba	N
RGV_GO4	*Leptogorgia*	RGV Reef	17/08/21	26.1645960	-97.0247440	Scuba	N
RGV_GO5	*Leptogorgia*	RGV Reef	17/08/21	26.1645960	-97.0247440	Scuba	N
SPJ2_B30	*Leptogorgia virgulata*	SPI Jetty	30/07/17	26.0674830	-97.1504410	Scuba	Y
7261_A01	*Leptogorgia virgulata*	Oil Rig	08/06/17	27.3835000	-96.1455200	Scuba	Y
LIB1_A04	*Leptogorgia virgulata*	Liberty Platforms	02/09/16	26.4296780	-97.0241160	Scuba	Y
LIB2_A05	*Leptogorgia virgulata*	Liberty Ship	12/12/14	26.4296670	-97.0243380	Scuba	Y
PIS1_A01	*Leptogorgia virgulata*	Port Isabel	03/06/14	26.0674830	-97.1504410	Scuba	Y
DFH32-523A	*Ellisella* clade 2a	McGrail Bank	24/09/17	27.9993640	-92.6187360	ROV	N
DFH37-653E	*Bebryce cinerea*	Parker Bank	09/07/18	28.0831911	-92.0143360	ROV	N
DFH37-669C	*Bebryce cinerea*	Rezak Bank	09/09/18	27.9819656	-92.3951163	ROV	N
SBR1_B36	*Muricea pendulla*	Stetson Bank Rig	08/09/04	28.1722000	-94.2894670	ROV	N
DFH33-539A	*Muricea pendulla*	MacNeil Bank	29/09/17	28.0079550	-93.4799130	ROV	N
DFH36-648A	*Muricea pendulla*	Stetson Bank	30/07/18	28.1754481	-94.2933641	ROV	N

Table 1, Cont.

DFH36-648B	*Muricea pendulla*	Stetson Bank	30/07/18	28.1753603	-94.2933666	ROV	N
NHB2_A01	*Muricea pendulla*	N Hospital Bank	12/07/17	27.5774000	-96.4769000	ROV	N
SBR1_C37	*Muricea pendulla*	Stetson Bank Rig	08/09/04	28.1716070	-94.2896720	ROV	N
DFH32-505A	*Muricea pendulla*	Sonnier Bank	22/09/17	28.3481228	-92.4464145	ROV	N
HAB2_A02	*Muricea pendulla*	Harte Bank	27/09/12	26.6536601	-96.5745490	ROV	N
660A	*Muricea pendulla*	Parker Bank	09/08/18	27.9335030	-91.9541601	ROV	N
DFH32-519B	*Paracis* cf clade 2	McGrail Bank	24/09/17	27.9839040	-92.6217665	ROV	N
DFH32-508A	*Swiftia* sp.	Alderdice Bank	22/09/17	28.0951591	-92.0070240	ROV	N
669B	*Swiftia* sp.	Rezak Bank	09/09/18	27.9819405	-92.3951068	ROV	N
EFG1_B34	*Swiftia exserta*	E Flower Garden	08/09/04	27.8904620	-93.6148970	ROV	N
BRB1_A02	*Ellisella* sp. clade 2a	Bryant Bank	05/09/16	28.9897233	-92.4511383	ROV	N
DFH32-522A	*Paramuricea/Placogorgia* 1a	McGrail Bank	24/09/17	28.0113226	-92.6285790	ROV	N
DFH32-508B	*Paramuricea/Placogorgia* 1a	Alderdice Bank	22/09/17	28.0950453	-92.0061725	ROV	N
DFH32-516A	*Paramuricea/Placogorgia* 1a	McGrail Bank	24/09/17	27.9641951	-92.5553975	ROV	N
DFH32-530A	*Paramuricea/Placogorgia* 1a	Elvers Bank	25/09/17	27.8486895	-92.9014748	ROV	N
DFH33-548A	*Paramuricea/Placogorgia* 1a	Bright Bank	01/10/17	27.8506950	-93.2745200	ROV	N
DFH32-515B	*Paramuricea/Placogorgia* 1b	Alderdice Bank	22/09/17	28.0950453	-92.0061725	ROV	N
DFH33-543E	*Paramuricea/Placogorgia* 1b	Parker Bank	30/09/17	27.9210520	-92.0701220	ROV	N
DFH33-548B	*Paramuricea/Placogorgia* 1b	Bright Bank	01/10/17	27.8509350	-93.2747880	ROV	N
DFH35-634B	*Paramuricea/Placogorgia* 1b	Geyer Bank	25/07/18	27.7853020	-93.0697060	ROV	N
DFH37-656A	*Paramuricea/Placogorgia* 1b	Parker Bank	09/07/18	27.9609075	-91.9563718	ROV	N
DFH37-666A	*Placogorgia tenuis*	Rezak Bank	09/09/18	27.9564273	-92.3608181	ROV	N
HAB1_A01	*Paramuricea/Placogorgia* 1c	Harte Bank	24/09/16	26.6536110	-96.5727780	ROV	N
HAB1_A02	*Paramuricea/Placogorgia* 1c	Harte Bank	24/09/16	26.6536110	-96.5727780	ROV	N
HAB1_A06	*Paramuricea/Placogorgia* 1c	Harte Bank	24/09/16	26.6536110	-96.5727780	ROV	N
DFH37-671F	*Nicella*	Bouma Bank	09/10/18	28.0627250	-92.4618450	ROV	N
DFH32-515E	*Nicella*	McGrail Bank	23/09/17	27.9510035	-92.5428005	ROV	N
DFH32-515M	*Nicella*	McGrail Bank	23/09/17	27.9510035	-92.5428005	ROV	N
DFH33-543J	*Nicella*	Parker Bank	30/09/17	27.9210520	-92.0701220	ROV	N
DFH33-543K	*Nicella*	Parker Bank	30/09/17	27.9210520	-92.0701220	ROV	N
DFH33-543L	*Nicella*	Parker Bank	30/09/17	27.9210520	-92.0701220	ROV	N

Table 1, Cont.

DFH33-543N	*Nicella*	Parker Bank	30/09/17	27.9210520	-92.0701220	ROV	N
DFH33-551B	*Nicella*	Bright Bank	01/10/17	27.8323000	-93.4169000	ROV	N
DFH32-518B	*Callogorgia*	McGrail Bank	24/09/17	27.9840725	-92.6042420	ROV	N
DFH32-535B	*Callogorgia*	Elvers Bank	25/09/17	27.8428331	-92.8762400	ROV	N
DFH37-657F	*Callogorgia*	Parker Bank	09/08/18	27.9638900	-91.9973951	ROV	N
DFH37-657H	*Callogorgia*	Parker Bank	09/08/18	27.9632065	-91.9991846	ROV	N
LIB4_A01	*Leptogorgia hebes*	Liberty Platforms	20/03/17	26.4200000	-97.0240000	Scuba	N
PIS1_A02	*Leptogorgia hebes*	Port Isabel	03/06/14	26.0674830	-97.1504410	Scuba	N
SPJ2_B45	*Leptogorgia hebes*	SPI Jetty	30/07/17	26.0674830	-97.1504410	Scuba	N
SPJ2_B46	*Leptogorgia hebes*	SPI Jetty	30/07/17	26.0674830	-97.1504410	Scuba	N
SPJ2_B48	*Leptogorgia hebes*	SPI Jetty	30/07/17	26.0674830	-97.1504410	Scuba	N
USNM1550647	*Placogorgia sp.*	NE of Mona	13/11/18	18.2082000	-67.8018000	ROV	N
USNM1583145	*Bebryce grandis*	Madison Swanson	20/09/11	29.1826000	-85.6820000	ROV	N
USNM1583205	*Thesea citrina*	Alabama Alps	26/09/11	29.1498000	-88.2020000	ROV	N
USNM1583232	*Bebryce cinerea*	Roughtongue Reef	28/06/14	29.4387000	-87.5763000	ROV	N
USNM1583234	*Scleracis* sp.	Roughtongue Reef	28/06/14	29.4386000	-87.5761000	ROV	N
USNM1583253	*Bebryce parastellata*	Roughtongue Reef	28/06/14	29.4392000	-87.5773000	ROV	N
USNM1583267	*Placogorgia tenuis*	Coral Trees Reef	06/07/14	29.5047000	-86.1458000	ROV	N
USNM1583271	*Thesea rubra*	Coral Trees Reef	06/07/14	29.4939000	-86.1471000	ROV	N
USNM1583277	*Thesea parviflora*	Madison Swanson	09/07/14	29.1850000	-85.6799000	ROV	N
USNM1583284	*Scleracis* sp.	Madison Swanson	09/07/14	29.1929000	-85.6753000	ROV	N

Table 2. Data Analysis Variables

Analysis information for 98 octocoral samples used in this study. This includes unique shortened sample ID, octocoral group, collection site, depth in meters, collection season, reef type collected from, and whether the sample was collected from the Flower Garden Banks or South Texas Banks region. Note Table 1 for full sample ID.

Sample ID	Group	Location	Depth (m)	Season	Reef Type	Region
1550647	*Placogorgia*	NE of Mona	504	Fall	Natural	NA
1583145	*Bebryce*	Madison Swanson	85	Fall	Natural	NA
1583205	*Thesea*	Alabama Alps	87	Fall	Natural	NA
1583232	*Bebryce*	Roughtongue Reef	62	Summer	Natural	NA
1583234	*Scleracis*	Roughtongue Reef	61	Summer	Natural	NA
1583253	*Bebryce*	Roughtongue Reef	59	Summer	Natural	NA
1583267	*Placogorgia*	Coral Trees Reef	79	Summer	Natural	NA
1583271	*Thesea*	Coral Trees Reef	78	Summer	Natural	NA
1583277	*Thesea*	Madison Swanson	62	Summer	Natural	NA
1583284	*Scleracis*	Madison Swanson	64	Summer	Natural	NA
505A	*Muricea*	Sonnier Bank	58	Fall	Natural	Flower Garden Banks
508A	*Swiftia*	Alderdice Bank	82	Fall	Natural	Flower Garden Banks
508B	*Paramuricea/Placogorgia*	Alderdice Bank	84	Fall	Natural	Flower Garden Banks
511C	*Thesea*	Alderdice Bank	66	Fall	Natural	Flower Garden Banks
511D	*Scleracis*	Alderdice Bank	66	Fall	Natural	Flower Garden Banks
515B	*Paramuricea/Placogorgia*	Alderdice Bank	125	Fall	Natural	Flower Garden Banks
515E	*Nicella*	McGrail Bank	125	Fall	Natural	Flower Garden Banks
515L	*Scleracis*	McGrail Bank	125	Fall	Natural	Flower Garden Banks
515M	*Nicella*	McGrail Bank	125	Fall	Natural	Flower Garden Banks
516A	*Paramuricea/Placogorgia*	McGrail Bank	124	Fall	Natural	Flower Garden Banks
518B	*Callogorgia*	McGrail Bank	98	Fall	Natural	Flower Garden Banks
519B	*Paracis*	McGrail Bank	109	Fall	Natural	Flower Garden Banks
522A	*Paramuricea/Placogorgia*	McGrail Bank	98	Fall	Natural	Flower Garden Banks
523A	*Ellisella*	McGrail Bank	95	Fall	Natural	Flower Garden Banks

Table 2, Cont.

526B	*Scleracis*	Elvers Bank	154	Fall	Natural	Flower Garden Banks
530A	*Paramuricea/Placogorgia*	Elvers Bank	147	Fall	Natural	Flower Garden Banks
535B	*Callogorgia*	Elvers Bank	111	Fall	Natural	Flower Garden Banks
536A	*Thesea nivea*	MacNeil Bank	86	Fall	Natural	Flower Garden Banks
537A	*Scleracis*	MacNeil Bank	84	Fall	Natural	Flower Garden Banks
539A	*Muricea*	MacNeil Bank	86	Fall	Natural	Flower Garden Banks
543E	*Paramuricea/Placogorgia*	Parker Bank	133	Fall	Natural	Flower Garden Banks
543J	*Nicella*	Parker Bank	133	Fall	Natural	Flower Garden Banks
543K	*Nicella*	Parker Bank	133	Fall	Natural	Flower Garden Banks
543L	*Nicella*	Parker Bank	133	Fall	Natural	Flower Garden Banks
543N	*Nicella*	Parker Bank	112	Fall	Natural	Flower Garden Banks
546C	*Thesea*	Bright Bank	131	Fall	Natural	Flower Garden Banks
548A	*Paramuricea/Placogorgia*	Bright Bank	129	Fall	Natural	Flower Garden Banks
548B	*Paramuricea/Placogorgia*	Bright Bank	130	Fall	Natural	Flower Garden Banks
551B	*Nicella*	Bright Bank	140	Summer	Natural	Flower Garden Banks
634A	*Scleracis*	Geyer Bank	145	Summer	Natural	Flower Garden Banks
634B	*Paramuricea/Placogorgia*	Geyer Bank	97	Summer	Natural	Flower Garden Banks
635B	*Scleracis*	Bright Bank	90	Summer	Natural	Flower Garden Banks
640B	*Scleracis*	Bright Bank	90	Summer	Natural	Flower Garden Banks
640C1	*Scleracis*	Bright Bank	92	Summer	Natural	Flower Garden Banks
640D	*Thesea*	Stetson Bank	56	Summer	Natural	Flower Garden Banks
643A	*Thesea nivea*	Stetson Bank	57	Summer	Natural	Flower Garden Banks
643B	*Thesea nivea*	Stetson Bank	54	Summer	Natural	Flower Garden Banks
648A	*Muricea*	Stetson Bank	54	Summer	Natural	Flower Garden Banks
648B	*Muricea*	Stetson Bank	82	Fall	Natural	Flower Garden Banks
653C	*Thesea nivea*	Alderdice Bank	84	Fall	Natural	Flower Garden Banks
653E	*Bebryce*	Parker Bank	116	Fall	Natural	Flower Garden Banks
656A	*Paramuricea/Placogorgia*	Parker Bank	100	Fall	Natural	Flower Garden Banks
657D	*Scleracis*	Parker Bank	99	Fall	Natural	Flower Garden Banks
657F	*Callogorgia*	Parker Bank	99	Fall	Natural	Flower Garden Banks
657H	*Callogorgia*	Parker Bank	118	Fall	Natural	Flower Garden Banks
660C	*Thesea*	Parker Bank	126	Fall	Natural	Flower Garden Banks

Table 2, Cont.

666A	*Placogorgia*	Rezak Bank	124	Fall	Natural	Flower Garden Banks
669B	*Swiftia*	Rezak Bank	86	Fall	Natural	Flower Garden Banks
669C	*Bebryce*	Rezak Bank	86	Fall	Natural	Flower Garden Banks
671F	*Nicella*	Bouma Bank	64	Fall	Natural	Flower Garden Banks
7261_A01	*Leptogorgia*	Oil Rig	NA	Summer	Artificial	Flower Garden Banks
BRB1_A02	*Ellisella*	Bryant Bank	105	Fall	Natural	Flower Garden Banks
CLP1_B01	*Thesea nivea*	Clipper	NA	Summer	Artificial	South Texas Banks
CLP1_C02	*Thesea nivea*	Clipper	NA	Summer	Artificial	South Texas Banks
CLP2_A01	*Thesea nivea*	Clipper	31	Summer	Artificial	South Texas Banks
CLP2_A02	*Thesea nivea*	Clipper	31	Summer	Artificial	South Texas Banks
DFH37660A	*Muricea*	Parker Bank	118	Fall	Natural	Flower Garden Banks
DRB1_A01	*Scleracis*	Dream Bank	NA	Fall	Natural	South Texas Banks
DRB1_A03	*Scleracis*	Dream Bank	NA	Fall	Natural	South Texas Banks
DRB1_A04	*Paracis*	Dream Bank	NA	Fall	Natural	South Texas Banks
EFG1_B34	*Swiftia*	East Flower Garden Bank	89	Fall	Natural	Flower Garden Banks
H113_A08	*Thesea nivea*	High Island	NA	Summer	Artificial	Flower Garden Banks
HAB1_A01	*Paramuricea/Placogorgia*	Harte Bank	101	Fall	Natural	South Texas Banks
HAB1_A02	*Paramuricea/Placogorgia*	Harte Bank	107	Fall	Natural	South Texas Banks
HAB1_A06	*Paramuricea/Placogorgia*	Harte Bank	107	Fall	Natural	South Texas Banks
HAB2_A02	*Muricea*	Harte Bank	NA	Fall	Natural	South Texas Banks
LIB1_A04	*Leptogorgia*	Liberty Platforms	80	Fall	Artificial	South Texas Banks
LIB2_AO5	*Leptogorgia*	Liberty Ship	NA	NA	Artificial	South Texas Banks
LIB4_A01	*Leptogorgia*	Liberty Platforms	80	NA	Artificial	South Texas Banks
NHB1_A05	*Paracis*	N Hospital Bank	66	Summer	Natural	South Texas Banks
NHB1_A07	*Paracis*	N Hospital Bank	66	Summer	Natural	South Texas Banks
NHB1_A09	*Paracis*	N Hospital Bank	66	Summer	Natural	South Texas Banks
NHB1_A4	*Paracis*	N Hospital Bank	66	Summer	Natural	South Texas Banks
NHB2_A01	*Muricea*	N Hospital Bank	66	Summer	Natural	South Texas Banks
NHB2_A02	*Paracis*	N Hospital Bank	66	Summer	Natural	South Texas Banks
PIS1_A01	*Leptogorgia*	Port Isabel	NA	Summer	Artificial	South Texas Banks
PIS1_A02	*Leptogorgia*	Port Isabel	NA	Summer	Artificial	South Texas Banks
RGV_GO1	*Leptogorgia*	RGV Reef	NA	NA	Artificial	South Texas Banks

Table 2, Cont.

RGV_GO2	*Leptogorgia*	RGV Reef	NA	NA	Artificial	South Texas Banks
RGV_GO3	*Leptogorgia*	RGV Reef	NA	NA	Artificial	South Texas Banks
RGV_GO4	*Leptogorgia*	RGV Reef	NA	NA	Artificial	South Texas Banks
RGV_GO5	*Leptogorgia*	RGV Reef	NA	NA	Artificial	South Texas Banks
SBR1_B36	*Muricea*	Stetson Bank Rig	54	Fall	Artificial	Flower Garden Banks
SBR1_C37	*Muricea*	Stetson Bank Rig	53	Fall	Artificial	Flower Garden Banks
SPJ2_B30	*Leptogorgia*	SPI Jetty	5	Summer	Artificial	South Texas Banks
SPJ2_B45	*Leptogorgia*	SPI Jetty	5	Summer	Artificial	South Texas Banks
SPJ2_B46	*Leptogorgia*	SPI Jetty	5	Summer	Artificial	South Texas Banks
SPJ2_B48	*Leptogorgia*	SPI Jetty	5	Summer	Artificial	South Texas Banks

Table 3. Alpha Diversity Value (Full Sample Set)

Alpha diversity (Shannon index) values for 13 octocoral groups in full high-read dataset. Values are presented as means ± standard error of mean.

Octocoral Group	**Alpha Diversity**
Bebryce	5.616 ± 0.095
Callogorgia	3.225 ± 0.512
Ellisella	2.184 ± 0.506
Leptogorgia	3.066 ± 0.201
Muricea	2.405 ± 0.174
Nicella	2.193 ± 0.392
Paracis	1.926 ± 0.193
Paramuricea/Placogorgia	2.711 ± 0.344
Placogorgia	1.817 ± 0.142
Scleracis	2.256 ± 0.297
Swiftia	1.288 ± 0.259
Thesea	1.812 ± 0.128
Thesea nivea	5.166 ± 0.103

Table 4. Pairwise Wilcoxon Rank Sum Test on Alpha Diversity (Full Sample Set)

Pairwise Wilcoxon rank sum test with Benjamini-Hochberg adjusted p-values for all 13 octocoral groups.

	Bebryce	***Callogorgia***	***Ellisella***	***Leptogorgia***	***Muricea***	***Nicella***	***Paracis***
Callogorgia	0.04747	-	-	-	-	-	-
Ellisella	0.19048	0.68197	-	-	-	-	-
Leptogorgia	0.00195	0.95741	0.43285	-	-	-	-
Muricea	0.00708	0.20083	0.95806	0.07474	-	-	-
Nicella	0.00910	0.20083	0.84040	0.04747	0.23033	-	-
Paracis	0.01159	0.06520	0.95741	0.00717	0.12046	0.98022	-
Paramuricea/Placogorgia	0.00910	0.49696	0.71889	0.38839	0.95741	0.40268	0.20222
Placogorgia	0.08342	0.12046	0.92313	0.02012	0.19500	0.95806	0.94203
Scleracis	0.00202	0.22086	1.00000	0.06579	0.57967	0.83640	0.78323
Swiftia	0.08342	0.12046	0.54737	0.01159	0.05065	0.30872	0.29792
Thesea	0.01159	0.02364	0.65000	0.00202	0.04747	0.95741	0.92313
Thesea nivea	0.04065	0.01212	0.08342	0.00012	0.00107	0.00195	0.00195
	Paramuricea/Placogorgia	***Placogorgia***	***Scleracis***	***Swiftia***	***Thesea***		
Callogorgia	-	-	-	-	-	-	-
Ellisella	-	-	-	-	-	-	-
Leptogorgia	-	-	-	-	-	-	-
Muricea	-	-	-	-	-	-	-
Nicella	-	-	-	-	-	-	-
Paracis	-	-	-	-	-	-	-
Paramuricea/Placogorgia	-	-	-	-	-	-	-
Placogorgia	0.37329	-	-	-	-	-	-
Scleracis	0.48509	0.75612	-	-	-	-	-
Swiftia	0.04643	0.54737	0.20083	-	-	-	-
Thesea	0.16650	1.00000	0.64175	0.20222	-	-	-
Thesea nivea	0.00304	0.03223	0.00063	0.03223	0.00195	-	-

Table 5. PERMANOVA Results on Microbiome Drivers

PERMANOVA on Bray-Curtis distances with standard 999 permutations and ordered by terms for full (n=98) octocoral dataset analyzing Octocoral Group, Reef Type, Region, and Season.

	Degrees of Freedom	Sum of Squares	R2	F	Pr (>F)
Octocoral Group	12	21.876	0.49153	6.8473	0.001
Reef Type	1	2.377	0.05342	5.4174	0.001
Region	1	1.781	0.04478	4.0319	0.001
Season	1	1.277	0.03111	2.8582	0.002

Table 6. Top Three Most Predominant Microbial Class per Octocoral Group

The top three most abundant microbial classes with percentage of total microbiome composition for each of the 13 octocoral groups (n = 98, samples rarified to even sequence depth of 7621).

Octocoral Group	**Class 1**	**Class 2**	**Class 3**
Bebryce	Gammaproteobacteria (29.9%)	Alphaproteobacteria (18.8%)	Bacteroidia (8.9%)
Callogorgia	Gammaproteobacteria (44.6%)	Nitrososphaeria (11.8%)	Fibrobacteria (7.9%)
Ellisella	Gammaproteobacteria (77.9%)	Mollicutes (10.7%)	Bacilli (2.4%)
Leptogorgia	Gammaproteobacteria (27.0%)	Nitrososphaeria (21.1%)	Mollicutes (18.3%)
Muricea	Gammaproteobacteria (38.6%)	Spirochaetia (27.1%)	Alphaproteobacteria (11.3%)
Nicella	Gammaproteobacteria (61.9%)	Nitrososphaeria (15.1%)	Nitrospira (4.2%)
Paracis	Gammaproteobacteria (50.0%)	Mollicutes (40.3%)	Alphaproteobacteria (2.9%)
Paramuricea/Placogorgia	Gammaproteobacteria (32.7%)	Mollicutes (16.2%)	Nitrososphaeria (15.3%)
Placogorgia	Gammaproteobacteria (51.7%)	Clostridia (19.5%)	Alphaproteobacteria (14.0%)
Scleracis	Gammaproteobacteria (43.4%)	Mollicutes (25.1%)	Nitrososphaeria (17.7%)
Swiftia	Gammaproteobacteria (45.1%)	Nitrososphaeria (43.8%)	Alphaproteobacteria (3.3%)
Thesea	Mollicutes (35.9%)	Gammaproteobacteria (33.5%)	Nitrososphaeria (12.3%)
Thesea nivea	Gammaproteobacteria (36.5%)	Alphaproteobacteria (19.5%)	Bacteroidia (9.0%)

Table 7. Alpha Diversity Values (High and Low Read Datasets)

Alpha diversity (Shannon index) values for 5 octocoral species (n = 5 for all except n=4 for Paracis cf. enopla clade 1) in low and high sequence dataset. Values are presented as means ± standard error of mean.

Octocoral Group	**Low Sequence Depth Alpha Diversity**	**High Sequence Depth Alpha Diversity**
Leptogorgia virgulata	1.842 ± 0.172	2.465 ± 0.208
Scleracis (Red)	1.663 ± 0.318	1.836 ± 0.156
Paracis cf. enopla clade 1	1.623 ± 0.189	1.818 ± 0.141
Scleracis (Yellow)	1.379 ± 0.500	1.938 ± 0.478
Thesea nivea	4.616 ± 0.122	5.174 ± 0.095

Table 8. Pairwise Wilcoxon Rank Sum Test on Alpha Diversity (High Read Dataset)

Pairwise Wilcoxon rank sum test with Benjamini-Hochberg adjusted p-values for 5 high-read dataset octocoral species (n = 5 for all except n=4 for Paracis cf. enopla clade 1) on alpha diversity (Shannon index) values.

	Leptogorgia virgulata	***Paracis* cf. *enopla* clade 1**	***Scleracis* (Red)**	***Scleracis* (Yellow)**
Paracis cf. *enopla* clade 1	0.106			
Scleracis (Red)	0.106	1.000		
Scleracis (Yellow)	0.782	1.000	1.000	
Thesea nivea	0.026	0.040	0.026	0.026

Table 9. Pairwise Wilcoxon Rank Sum Test on Alpha Diversity (Low Read Dataset)

Pairwise Wilcoxon rank sum test with Benjamini-Hochberg adjusted p-values for 5 low-read dataset octocoral species (n = 5 for all except n=4 for Paracis cf. enopla clade 1) on alpha diversity (Shannon index) values.

	Leptogorgia virgulata	***Paracis* cf. *enopla* clade 1**	***Scleracis* (Red)**	***Scleracis* (Yellow)**
Paracis cf. *enopla* clade 1	0.571			
Scleracis (Red)	0.935	1.000		
Scleracis (Yellow)	0.701	0.794	0.863	
Thesea nivea	0.026	0.040	0.026	0.026

Table 10. Top Three Most Predominant Microbial Genera per Octocoral Group

Top three most abundant microbial genera with percentage of total microbiome composition for each of the 13 octocoral groups (n = 98, samples rarified to even sequence depth of 7621).

Octocoral Group	**Genera 1 (Abundance%)**	**Genera 2 (Abundance%)**	**Genera 3 (Abundance%)**
Bebryce	*Spirochaeta* 2 (10.3%)	*Endozoicomonas* (10.2%)	*Candidatus* Nitrosopumilus (5.6%)
Callogorgia	*Endozoicomonas* (40.4%)	*Candidatus* Nitrosopumilus (12.7%)	Uncultured (9.6%)
Ellisella	Endozoicomonas (41.8%)	*Alteromonas* (26.2%)	*Mycoplasma* (12.4%)
Leptogorgia	*Candidatus* Nitrosopumilus (25.7%)	*Mycoplasma* (22.4%)	*Thiohalophilus* (11.8%)
Muricea	*Spirochaeta* 2 (30.9%)	*Endozoicomonas* (27.7%)	*Thiohalophilus* (8.8%)
Nicella	*Endozoicomonas* (57.9%)	*Candidatus* Nitrosopumilus (17.3%)	*Nitrospira* (4.8%)
Paracis	*Mycoplasma* (41.7%)	*Endozoicomonas* (31.0%)	*Thiohalophilus* (11.6%)
Paramuricea/Placogorgia	*Mycoplasma* (21.0%)	*Candidatus* Nitrosopumilus (18.8%)	BD1-7 clade (18.6%)
Placogorgia	BD1-7 clade (46.8%)	*Endozoicomonas* (23.5%)	*Candidatus* Nitrosopumilus (15.5%)
Scleracis	*Endozoicomonas* (40.5%)	*Mycoplasma* (26.7%)	*Candidatus* Nitrosopumilus (18.8%)
Swiftia	*Candidatus* Nitrosopumilus (45.5%)	*Endozoicomonas* (44.1%)	*Spiroplasma* (2.1%)
Thesea	*Mycoplasma* (35.8%)	*Endozoicomonas* (19.3%)	BD1-7 clade (12.9%)
Thesea nivea	*Endozoicomonas* (26.4%)	*Candidatus* Nitrosopumilus (7.4%)	*Spirochaeta* 2 (5.8%)

APPENDIX B

APPENDIX B

FIGURES

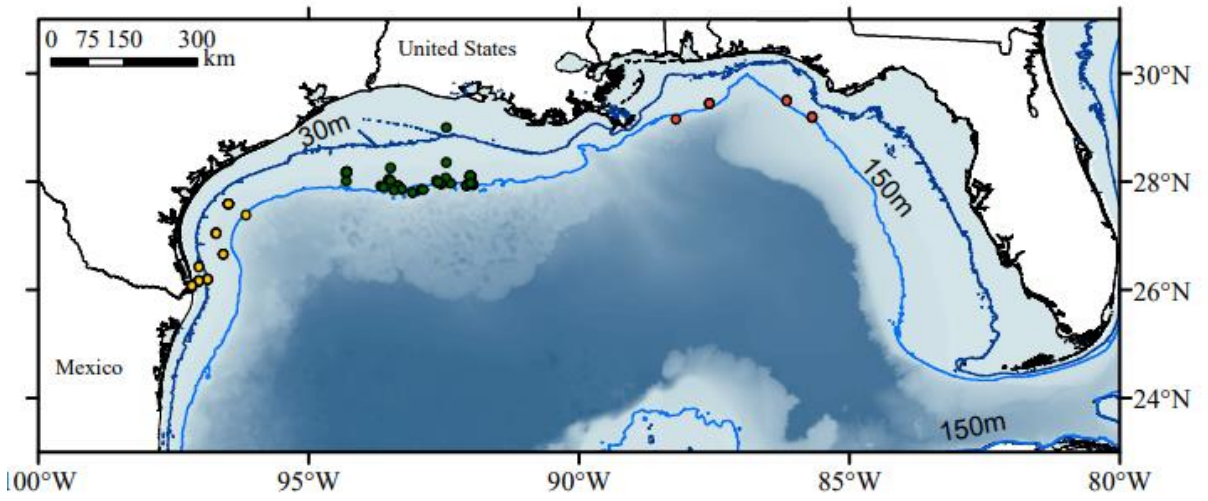

Figure 1. Map of Study Area

Study area showing western GoM banks for octocoral samples. STB (yellow), FGB (green), and USNM samples from eastern GoM mesophotic reefs (red) banks are shown. Each point represents a collection site, listed in Table 1. Lines denote 30 m (dark blue) and 150 m (light blue) bathymetric boundaries.

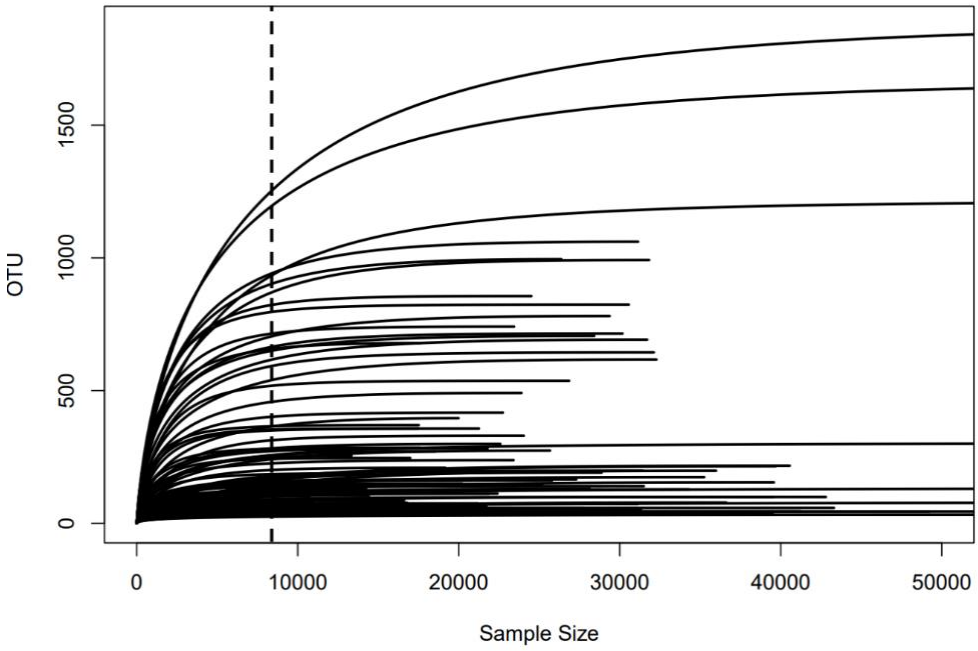

Figure 2. Rarefaction Curve (Full Sample Set)

Rarefaction curve for 98 octocoral samples. The vertical dashed line indicates sequence depth that samples were rarefied to (7621).

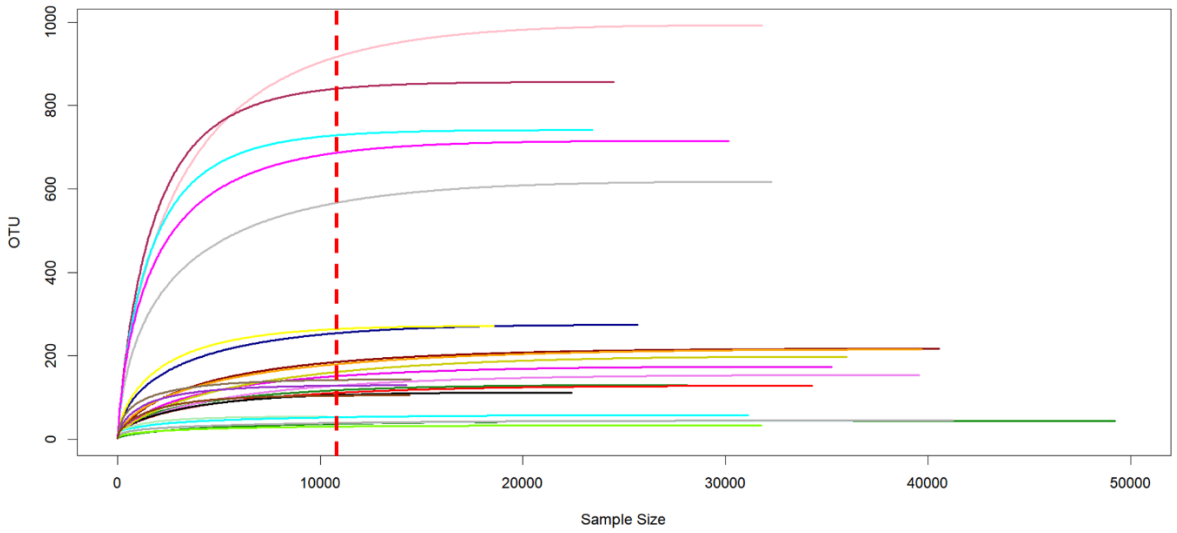

Figure 3A. Rarefaction Curve (High and Low Read Set)

Rarefaction curve for 24 preliminary octocoral samples at high sequence depth. The vertical dashed line indicates sequence depth that samples were rarefied to (10326).

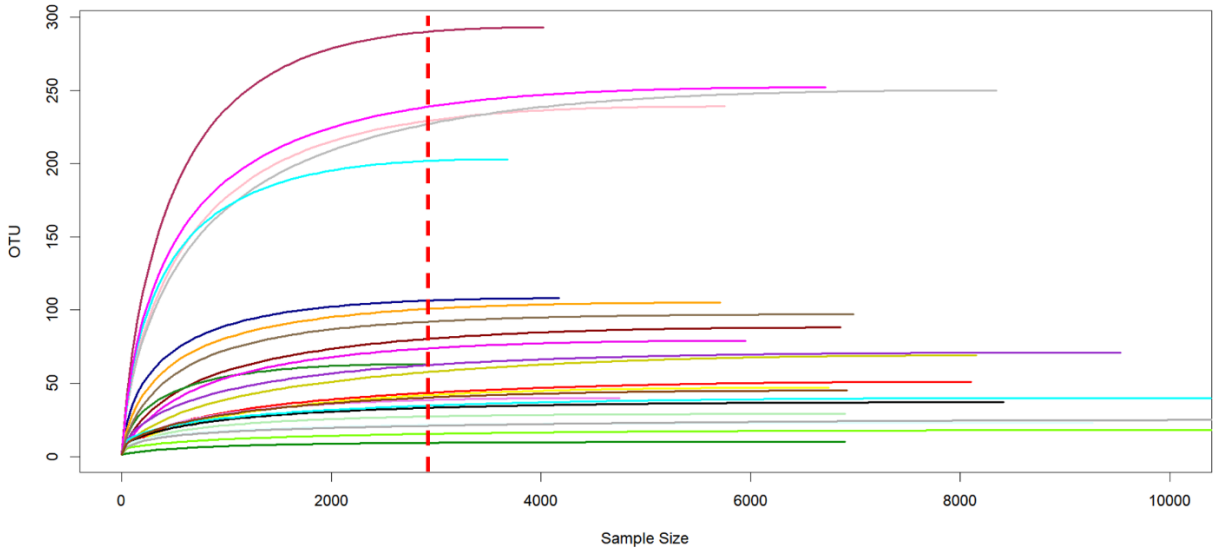

Figure 3B. Rarefaction curve for 24 preliminary octocoral samples at low sequence depth. The vertical dashed line indicates sequence depth that samples were rarefied to (2898).

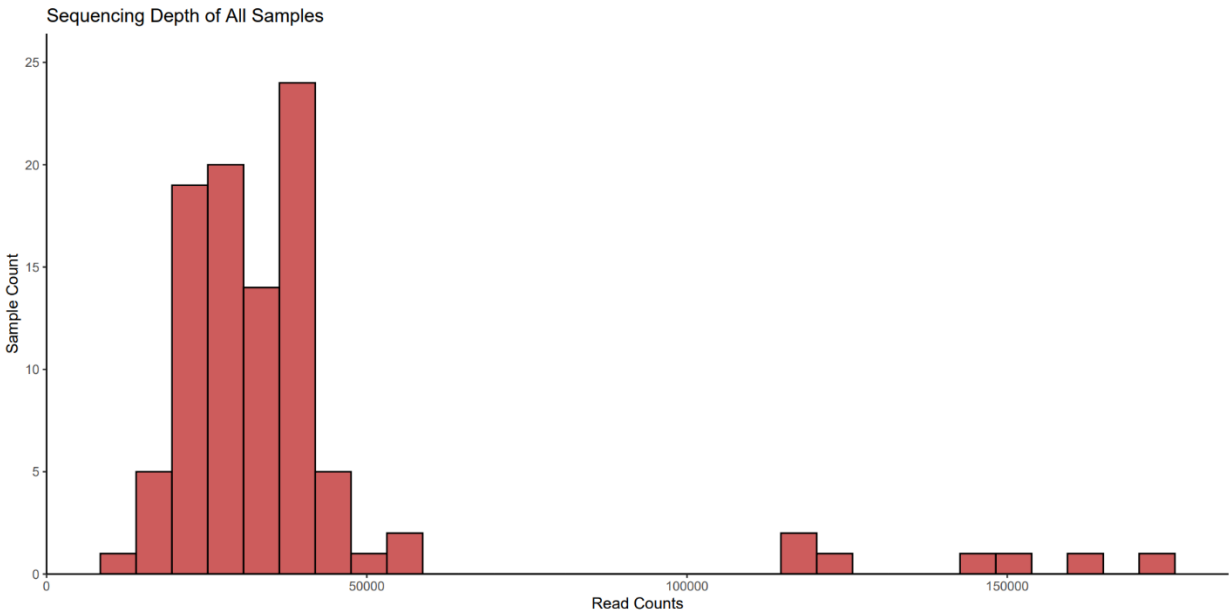

Figure 4A. Sequence Read Counts

Read counts of microbiome *16S* rRNA sequence run for all octocoral samples (n = 98).

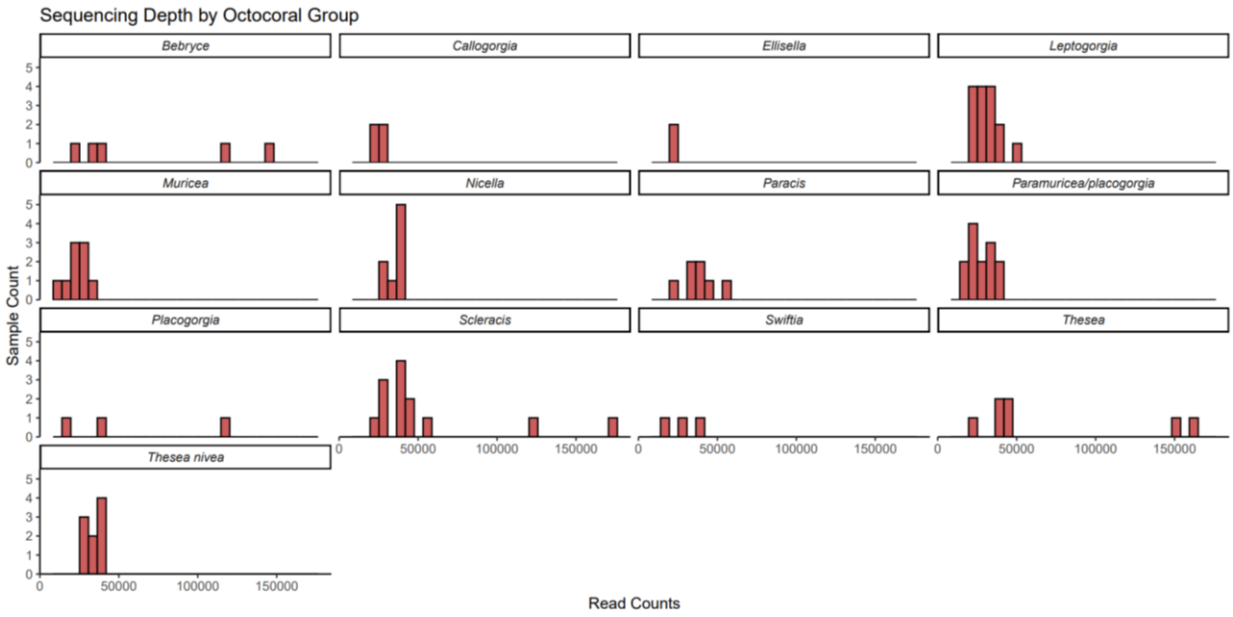

Figure 4B. Read counts of microbiome *16S* rRNA sequence run for all octocoral samples (n = 98) split by octocoral group (n = 13, Table 2)

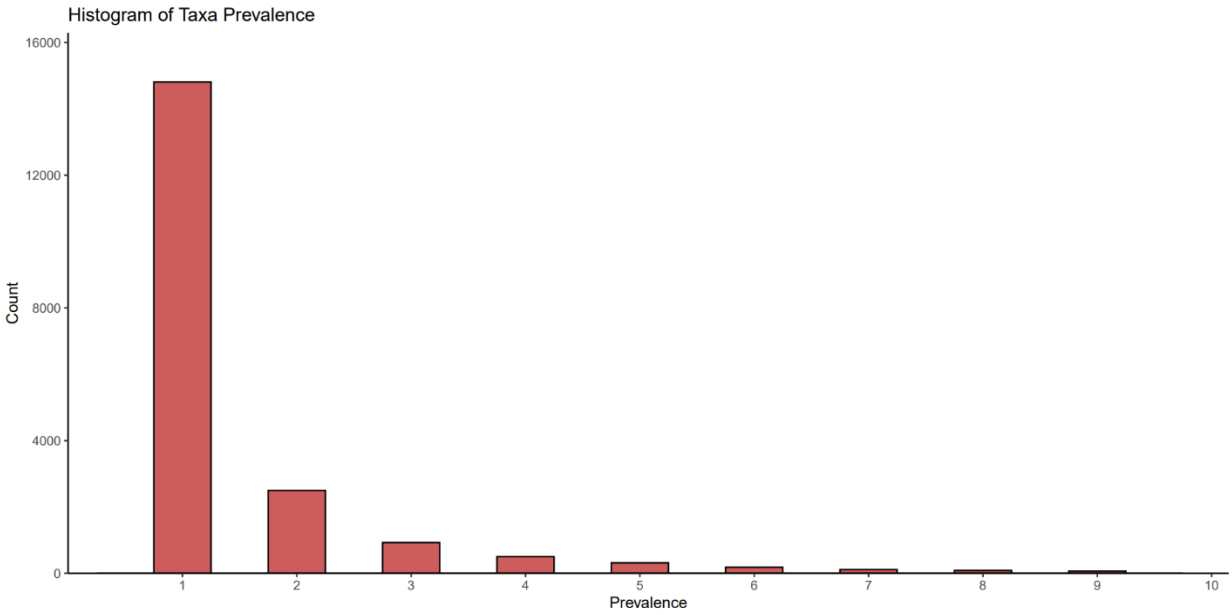

Figure 5. Number of Rare Microbial Taxa

Number of unique bacterial and archaeal taxa identified in octocoral samples (n = 98), indicating ~15000 taxa were unique to a single sample and that comparatively few taxa were found in two or more samples.

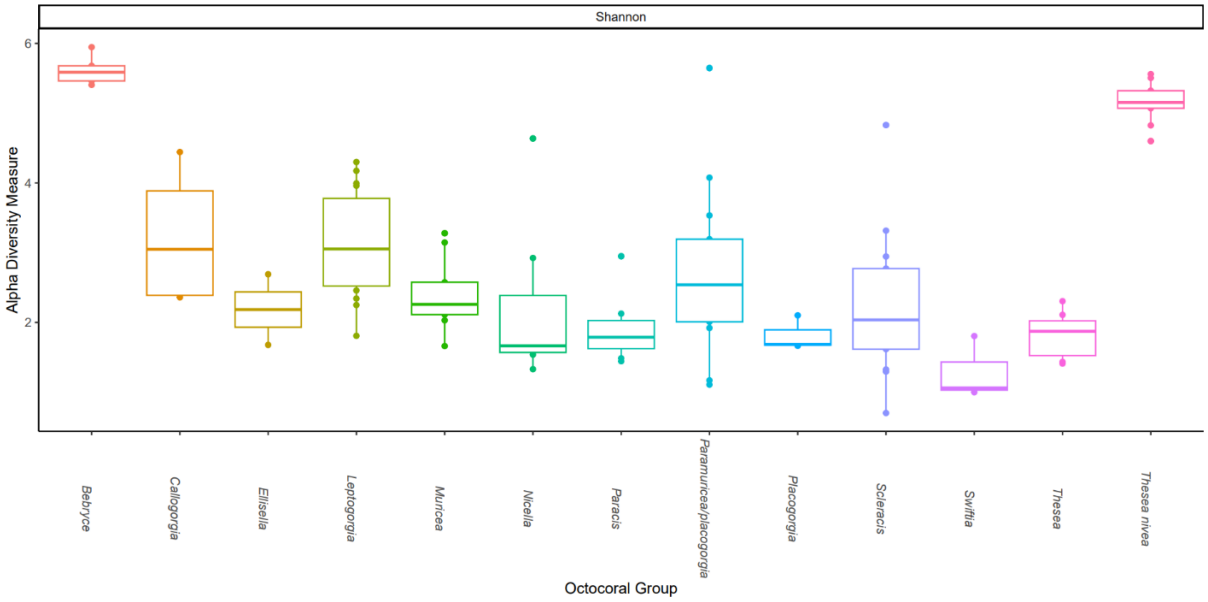

Figure 6A. Alpha Diversity (Full Sample Set)

Box plot showing alpha diversity using Shannon diversity index for each octocoral groups' microbiome for all 98 rarified samples. Bars represent standard error.

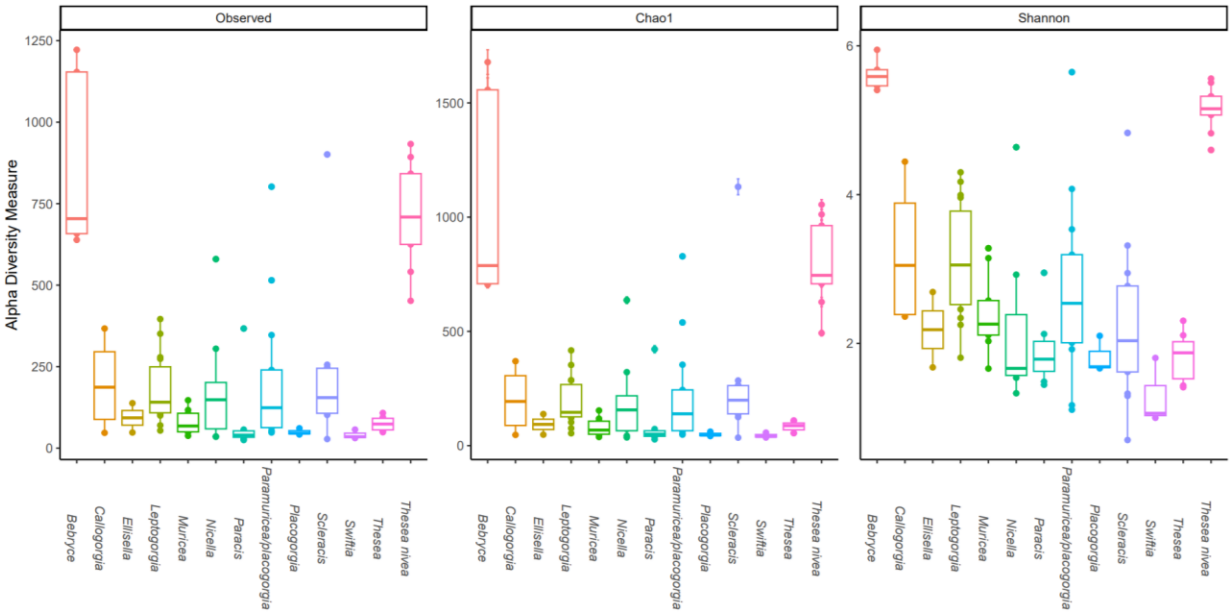

Figure 6B. Three box plots showing alpha diversity using Observed, Chao1, and Shannon indices respectively for all 98 rarified samples separated by octocoral group. Bars represent standard error.

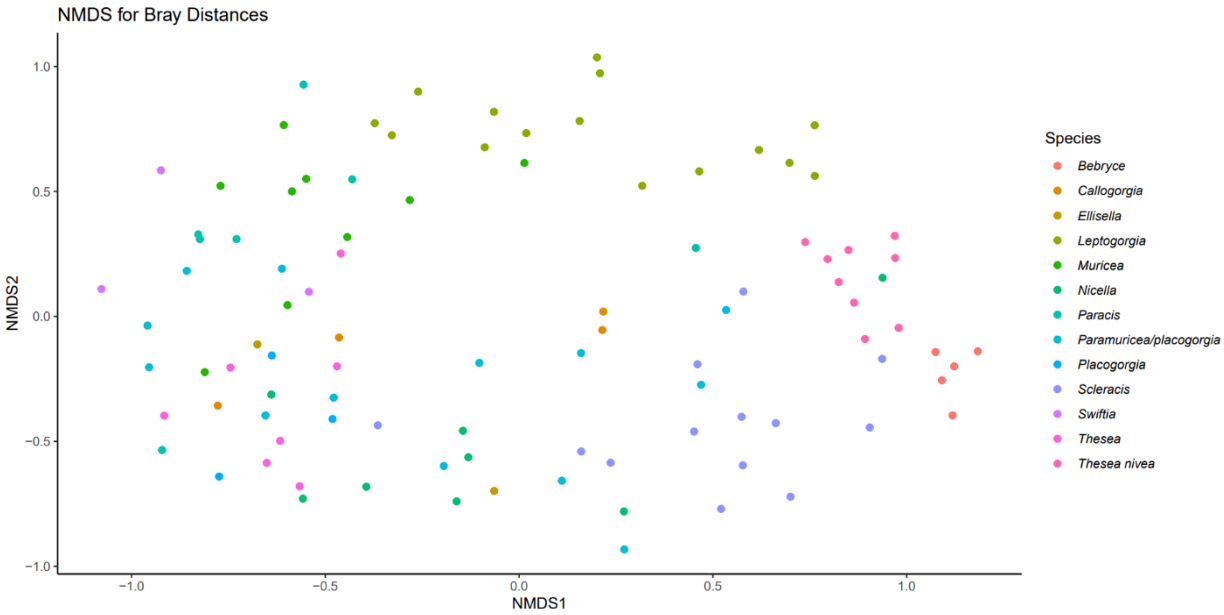

Figure 7. Octocoral Group nMDS

Non-metric multidimensional scaling (nMDS) ordination of Bray-Curtis distances between octocoral group microbiomes. Stress of 0.25.

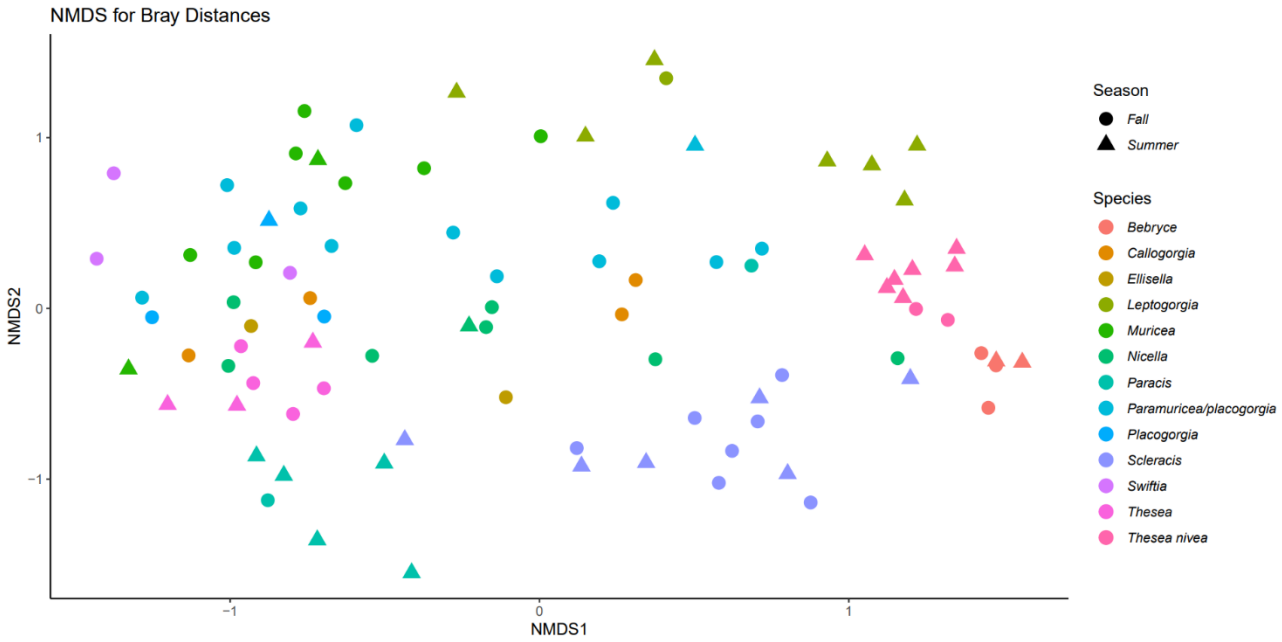

Figure 8. Seasonality nMDS

Non-metric multidimensional scaling (nMDS) ordination of Bray-Curtis distances between octocoral group microbiomes. Color indicates octocoral group while shape denotes season (Fall vs Summer). Stress of 0.25.

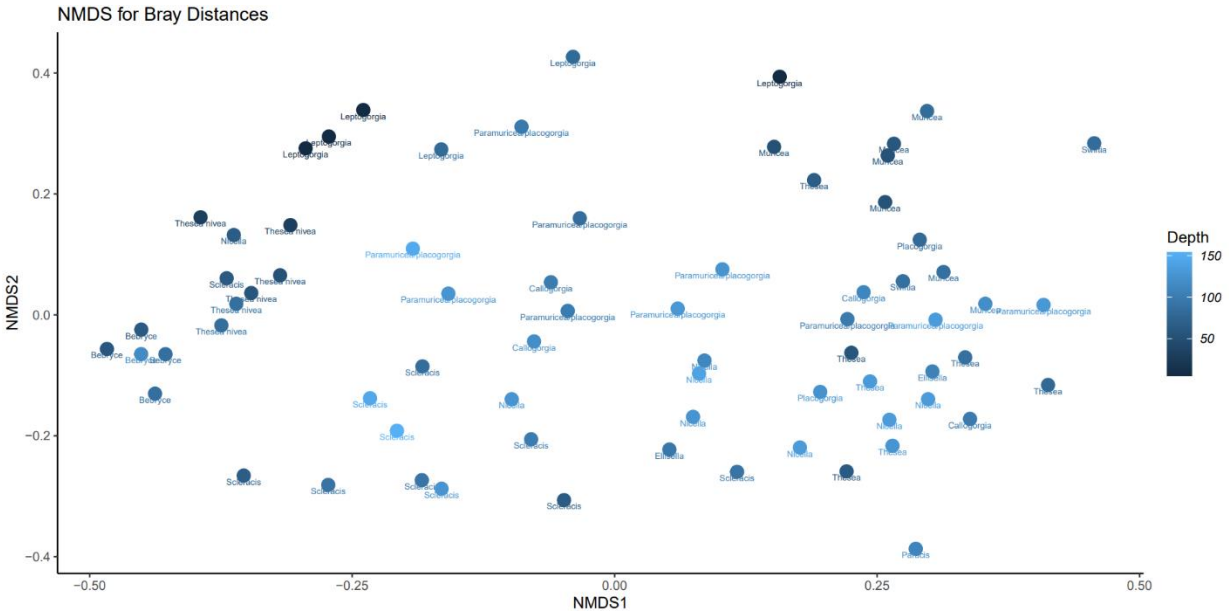

Figure 9. Depth nMDS

Non-metric multidimensional scaling (nMDS) ordination of Bray-Curtis distances between octocoral group microbiomes. Color indicates depth in meters while labels indicate octocoral group. Samples collected below 150 meters or with no depth data were omitted (n=17). Stress of 0.23.

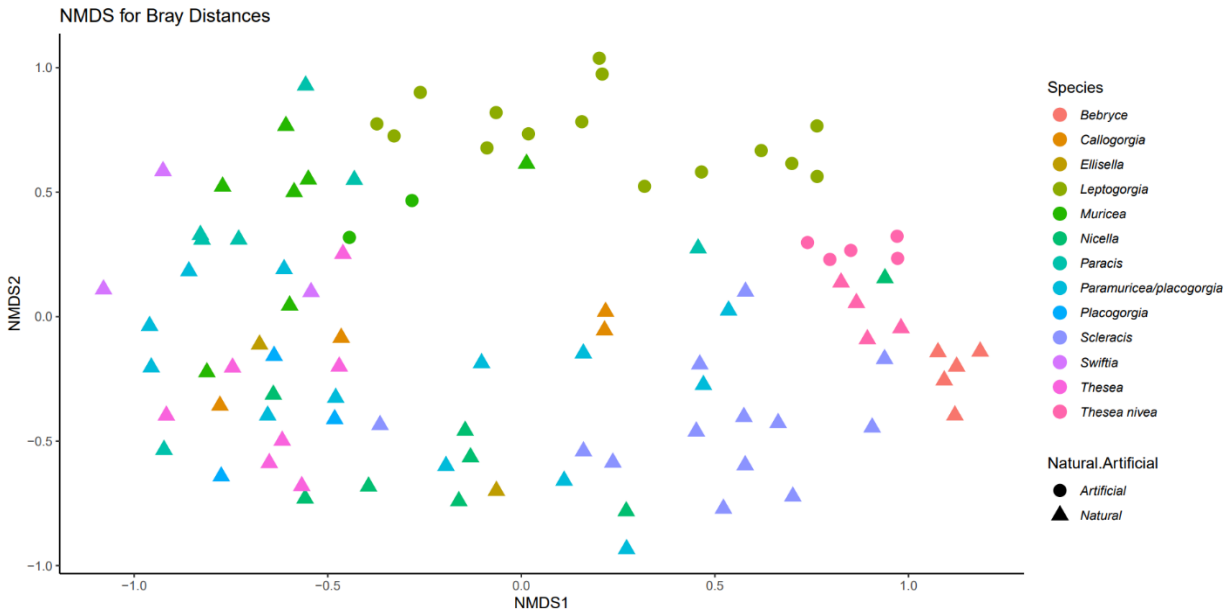

Figure 10. Reef Type nMDS

Non-metric multidimensional scaling (nMDS) ordination of Bray-Curtis distances between octocoral group microbiomes. Color indicates octocoral group while shape denotes reef type (Artificial vs Natural). Stress of 0.25.

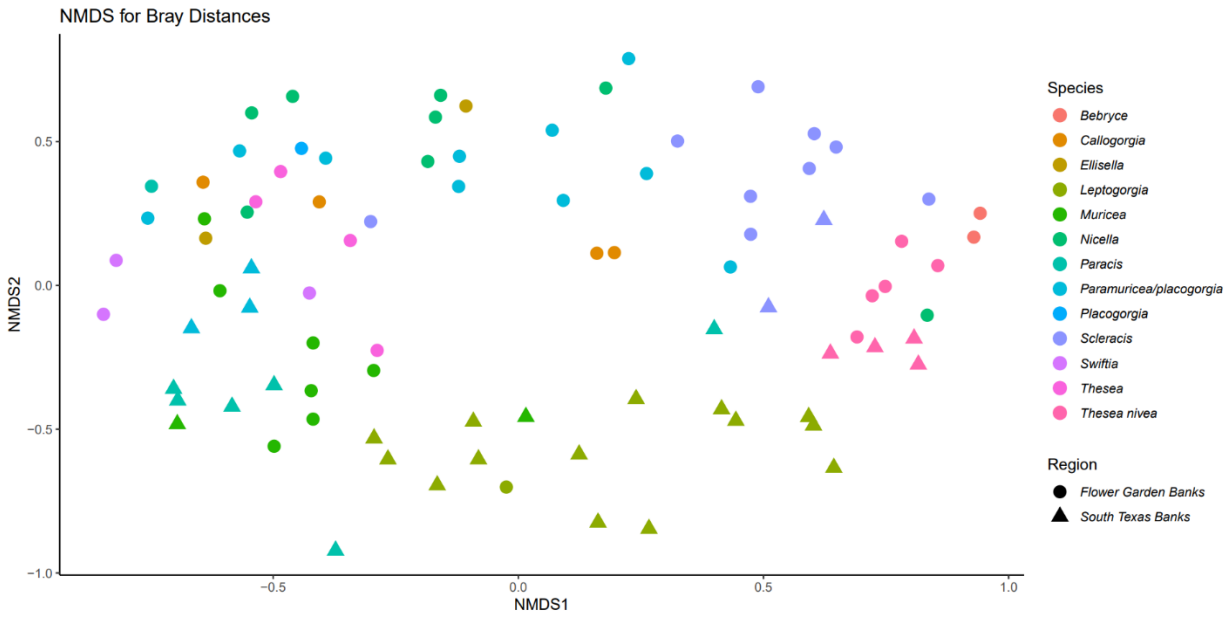

Figure 11. Sample Region nMDS

Non-metric multidimensional scaling (nMDS) ordination of Bray-Curtis distances between octocoral group microbiomes. Color indicates octocoral group while shape denotes sampling region (Flower Garden Banks vs South Texas Banks). Samples from outside these regions were omitted. Stress of 0.24.

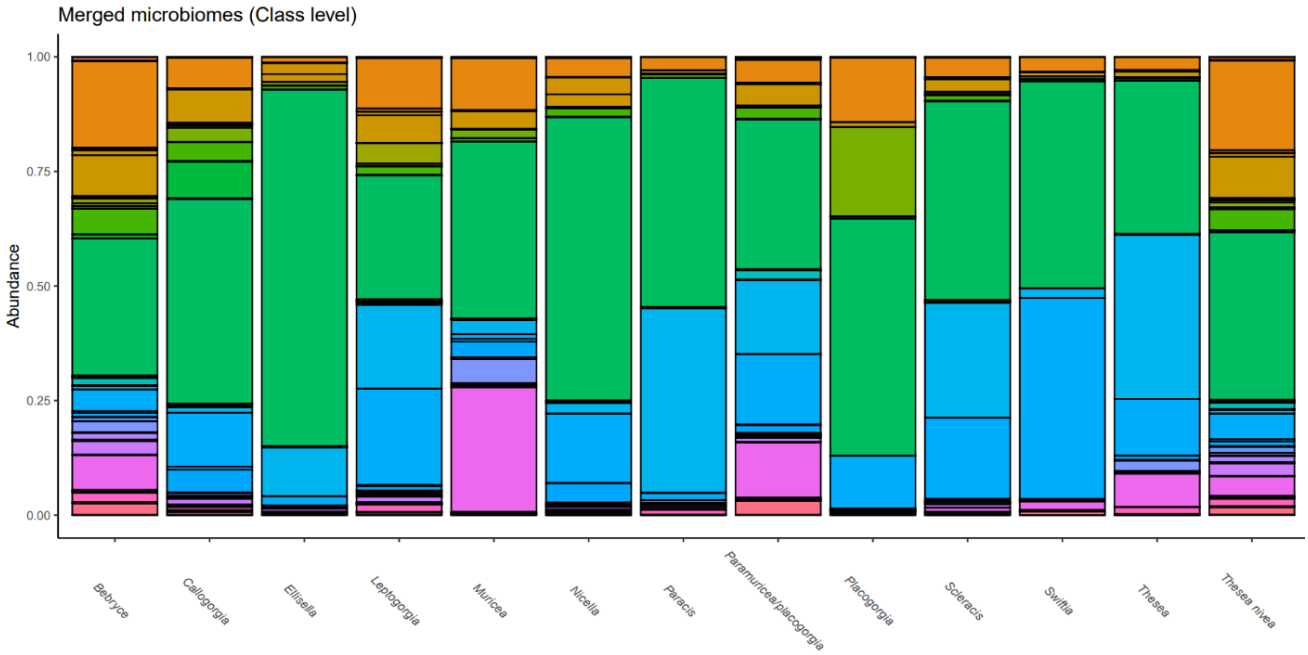

Figure 12A. Microbial Taxa (Class)

Taxonomic composition of merged microbiomes for each octocoral group at the class level. Bars represent merged microbiomes from all samples within each octocoral group as seen in Table 2.

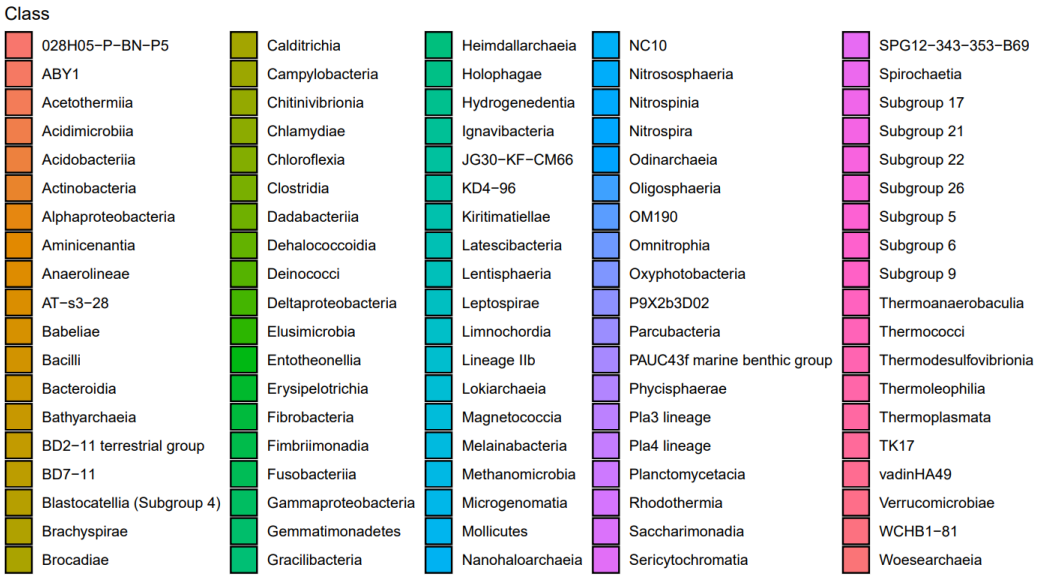

Figure 12B. Key for merged microbiomes.

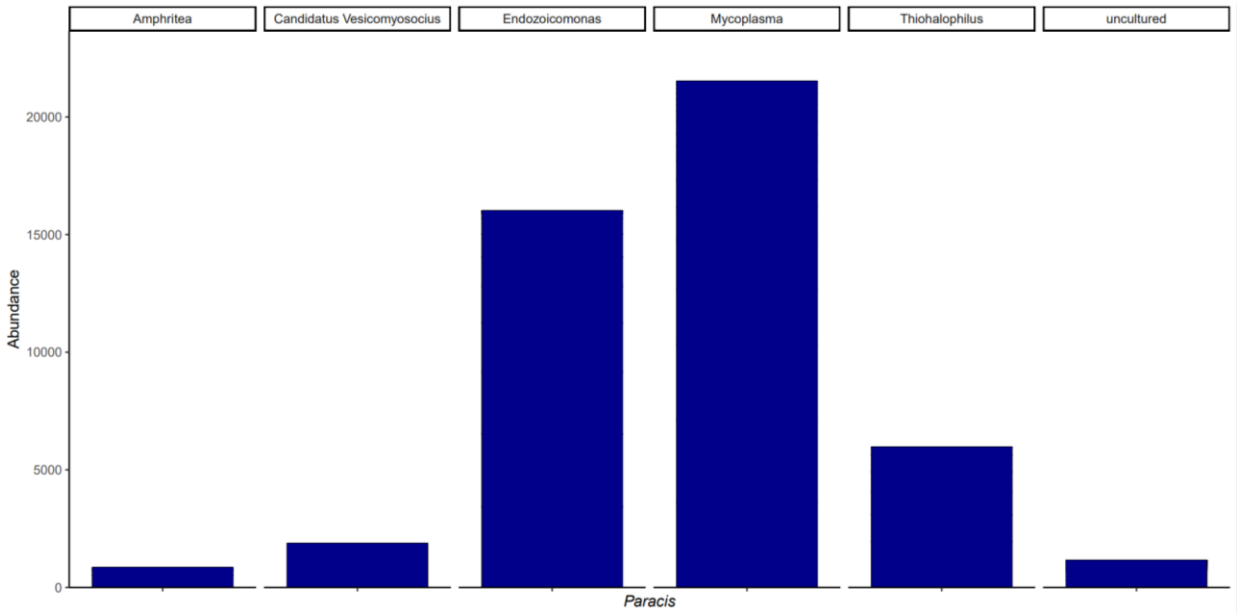

Figure 13A. Predominant Microbial Taxa (Genera)

Top six most abundant microbial genera within the microbiome of the octocoral genus *Paracis.*

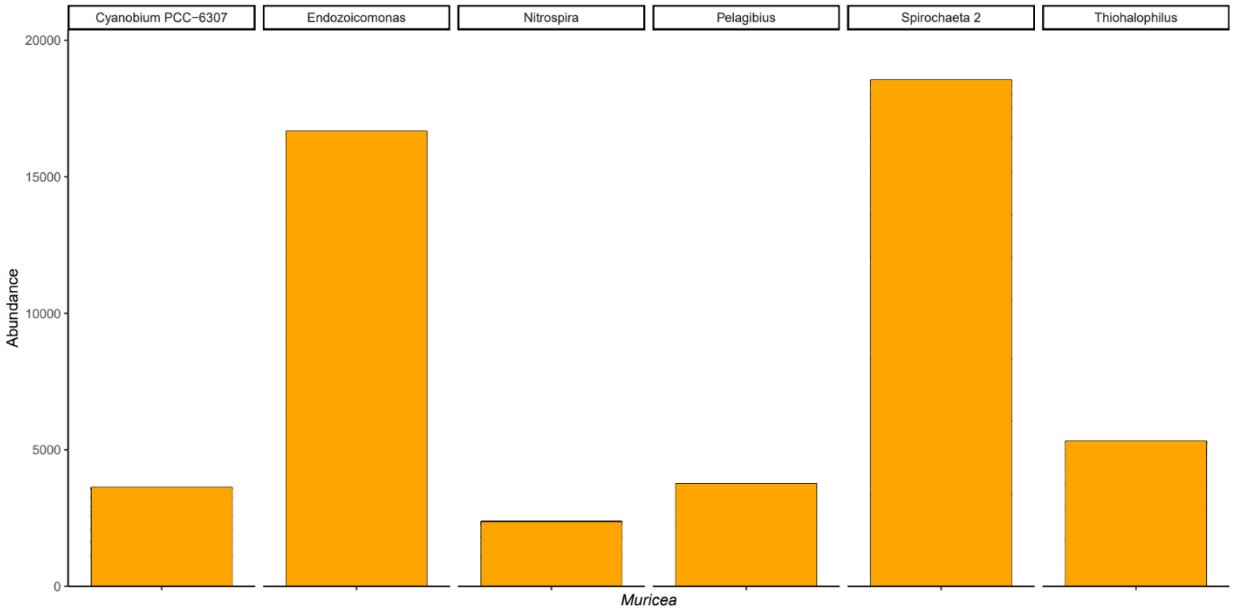

Figure 13B. Top six most abundant microbial genera within the microbiome of the octocoral genus *Muricea.*

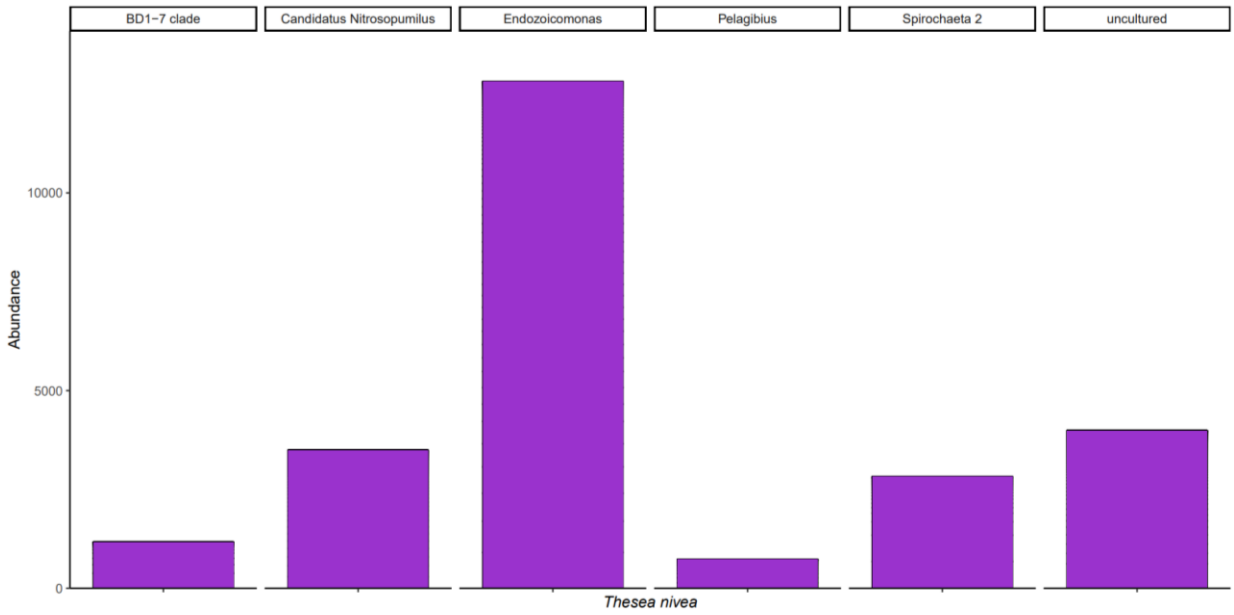

Figure 13C. Top six most abundant microbial genera within the microbiome of the octocoral group *Thesea nivea.*

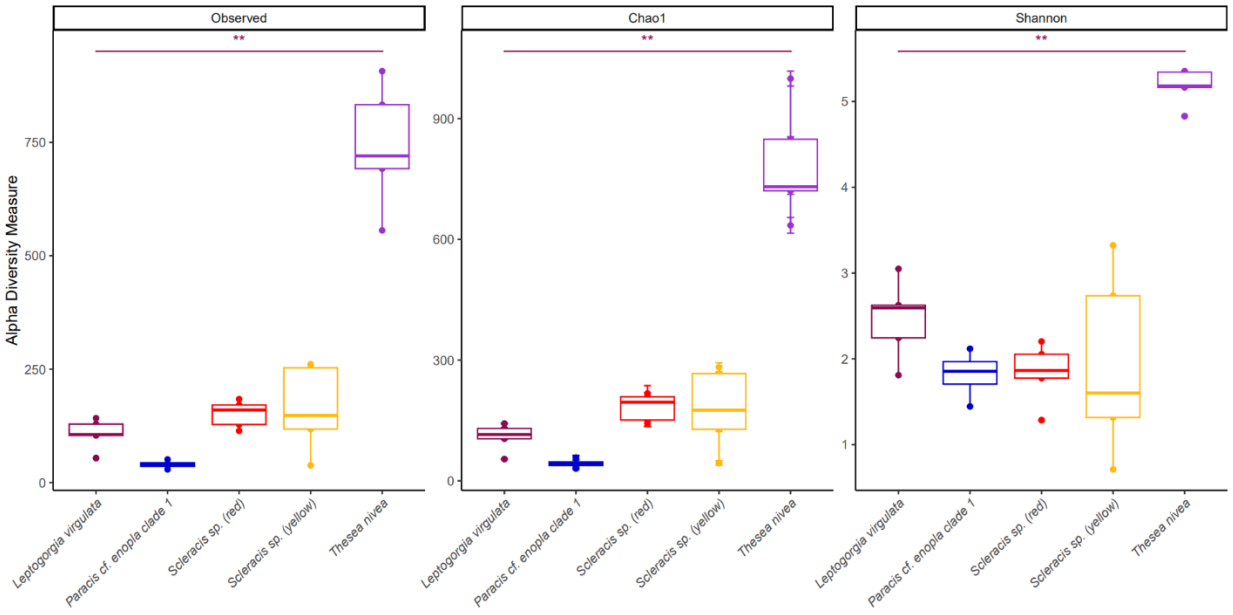

Figure 14A. Alpha Diversity (High and Low Read Set)

Three box plots showing Alpha diversity using Observed, Chao1, and Shannon indices respectively for the high read preliminary samples. Bars represent standard error.

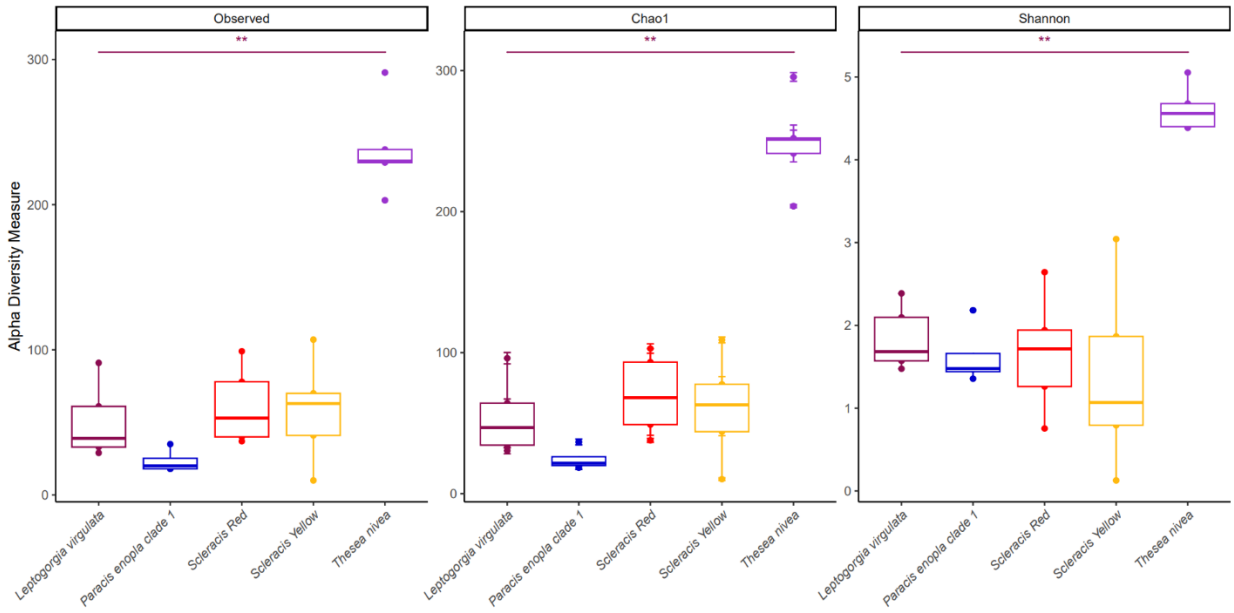

Figure 14B. Three box plots showing Alpha diversity using Observed, Chao1, and Shannon indices respectively for the low read preliminary samples. Bars represent standard error.

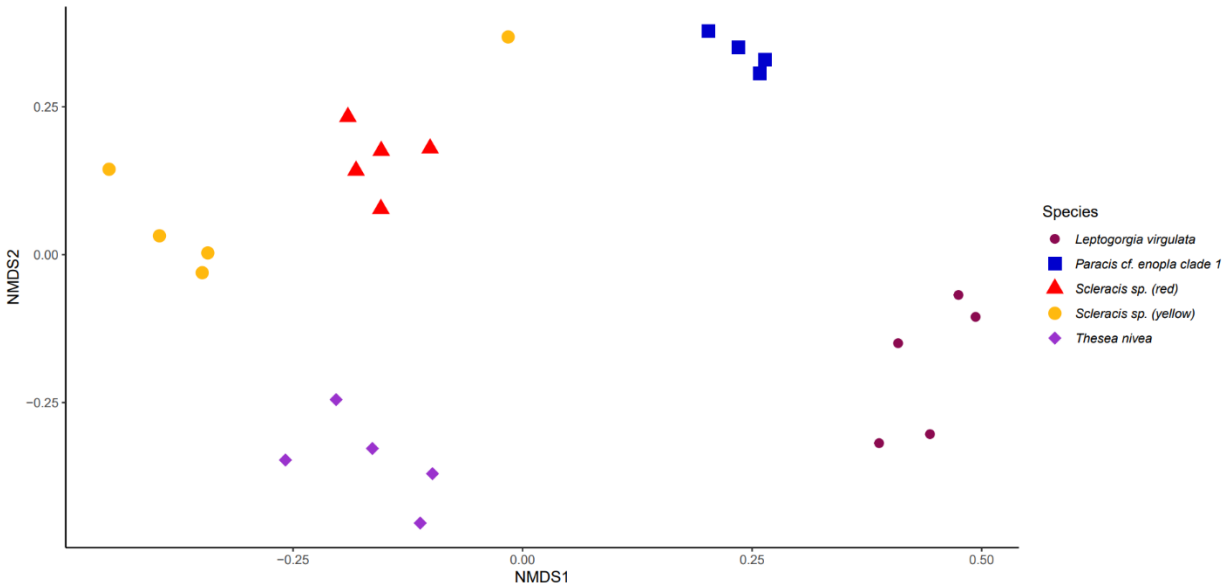

Figure 15A. High and Low Read nMDS

Non-metric multidimensional scaling (nMDS) ordination of Bray-Curtis distances between octocoral group microbiomes for high read samples. Stress of 0.129.

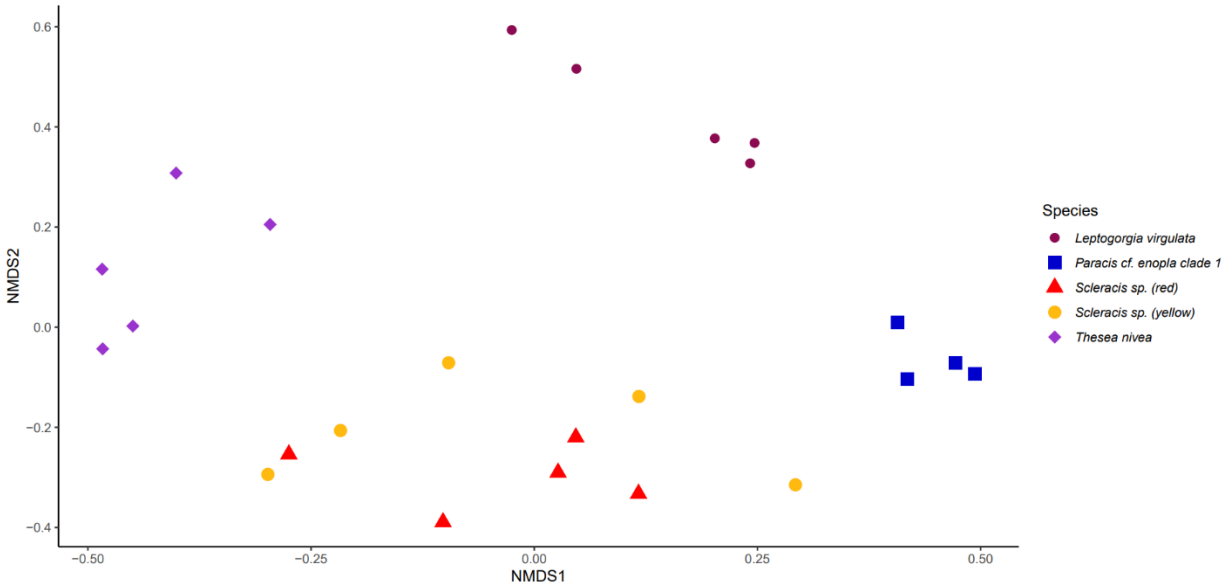

Figure 15B. Non-metric multidimensional scaling (nMDS) ordination of Bray-Curtis distances between octocoral group microbiomes for low read samples. Stress of 0.163.

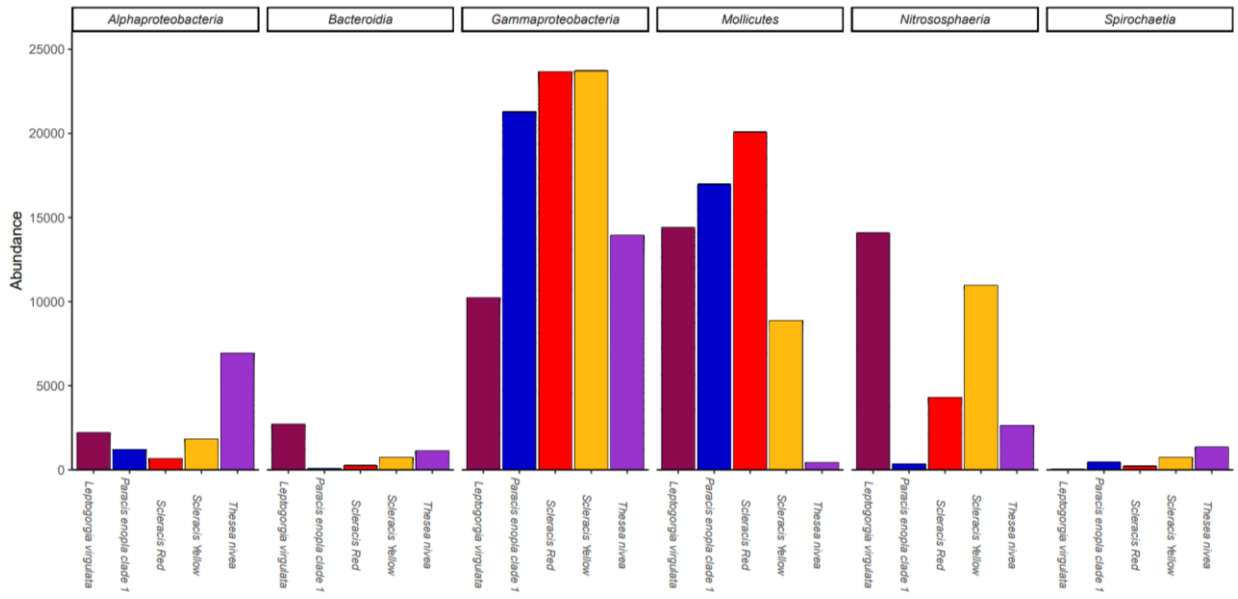

Figure 16A. Predominant Microbial Class (High and Low Read Set)

Top six most abundant microbial class in microbiomes of high-read preliminary samples.

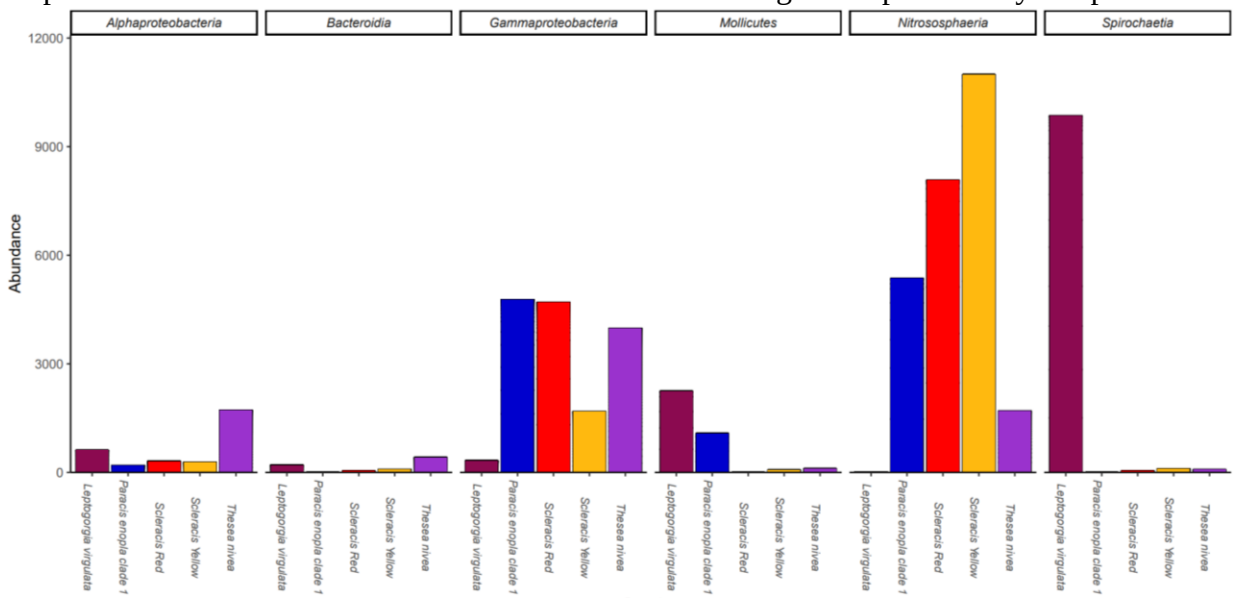

Figure 16B. Top six most abundant microbial class in microbiomes of low-read preliminary samples.

APPENDIX C

APPENDIX C

ANALYSIS CODE

Denoising

(QIIME2 denoise command) qiime dada2 denoise-paired

(Removal of chimera sequences) --p-chimera-method consensus \

(Filtering sequences shorter than 200bp) --p-trunc-len-f 200 --p-trunc-len-r 200 \

(Filtering sequences with maximum expected error higher than 2) --p-max-ee 2.0 \

Classifying

(ASVs referencing against the SILVA 132 using the classify-consensus-vsearch method) qiime feature-classifier classify-consensus-vsearch \

Phyloseq

(Merging of ASV counts, sample metadata, and ASV taxa into phyloseq object)

phyloseq(ASV_count, Metadata, Taxa_Table)

(Calculation of alpha diversity values for three different indices from phyloseq object)

microbiome::alpha(Phyloseq_object, index = "shannon", “chao1”, “observed”)

(Kruskal Wallis H test, to determine presence of significant differences between octocoral groups’ microbiomes alpha diversity)

kruskal.test(Alpha_diversity_values(Phyloseq_object)$Octocoral_group)

(Pairwise Wilcoxon Rank Sum test to determine which octocoral groups' microbiomes differ significantly from one another)

```
pairwise.wilcox.test(Alpha_diversity_values(Phyloseq_object)$Octocoral_group,
p.adjust.method = "BH")
```

(PERMANOVA code with 999 permutations using Bray Curtis distances)

```
adonis2(Phyloseq_object ~ Octocoral_group, data = Sample_Dataframe, permutations = 999,
method = "bray", by = "terms")
```

(nMDS ordination on Phyloseq object)

```
ord.nmds.bray <- ordinate(Phyloseq_object, method="NMDS", distance="bray")
```

BIOGRAPHICAL SKETCH

Edward (Ted) Gniffke graduated from Western Washington University in Bellingham, Washington where he earned a B.S. in Cell and Molecular Biology with a minor in Economics. From there he worked as a Chemist for Bio Rad before joining the Hawksbill Turtle Recovery Project at Hawai'i Volcano National Park. He then worked at the SEPS lab at Seattle Children's Research Institiute studying ASD proteomics and later COVID-19 virus. He joined the lab of Dr. Erin Easton as a graduate student (M.S. in Ocean, Coastal, and Earth Studies) in the School of Earth Environmental and Marine Sciences in July 2021 at University of Texas Rio Grande Valley. There he studied the microbiomes of mesophotic Octocorals sampled off of the western and northwestern Gulf of Mexico. Ted completed his Master of Science degree in August of 2023.

Edward (Ted) Gniffke can be contacted at ed.gniff@gmail.com or at his permanent mailing address of 4706 91st Ave SE Mercer Island, WA, 98040.